

Maria Luís Martins Barreira

**Pre-miR-29 as a lung cancer biopharmaceutical:
a new approach for its purification and delivery
with functionalized nanoparticles**

Dissertação de mestrado na área de Tecnologias do Medicamento
orientada pela Professora Doutora Ana Rita Figueiras e pela Professora Doutora Fani Sousa e
apresentada à Faculdade de Farmácia da Universidade de Coimbra

Setembro 2017



UNIVERSIDADE DE COIMBRA

**Pre-miR-29 as a lung cancer biopharmaceutical:
a new approach for its purification and delivery
with functionalized nanoparticles**

Maria Luís Martins Barreira

Dissertação de mestrado na área de Tecnologias do Medicamento orientada pela Professora Doutora Ana Rita Figueiras e pela Professora Doutora Fani Sousa e apresentada à Faculdade de Farmácia da Universidade de Coimbra

Setembro 2017



UNIVERSIDADE DE COIMBRA

Para os meus Pais...

Agradecimentos

Este ano foi um ano de grandes responsabilidades profissionais, de muitos momentos felizes, mas também de algumas adversidades. Assim, neste período final, chega a altura de agradecer às pessoas que contribuíram de diversas formas para a conclusão deste projeto. Primeiro, gostaria de agradecer à minha Orientadora Professora Doutora Ana Rita Figueiras, da Faculdade de Farmácia da Universidade de Coimbra, por me ter dado a oportunidade de integrar neste projeto tão aliciante. Obrigada pela sua orientação, disponibilidade, dedicação e por me proporcionar todas as condições necessárias para a conclusão deste trabalho. Devo também um agradecimento muito especial à minha Co-Orientadora Professora Doutora Fani Sousa, do Centro de Investigação em Ciências da Saúde da Universidade da Beira Interior, que me recebeu com tanta simpatia e por me ter "acolhido" tão amavelmente, durante todo este ano, ajudando-me no desenvolvimento do meu projeto de investigação. Queria agradecer-lhe, por nunca ter desistido de mim, por sempre me ter encorajado, por todo o seu vasto conhecimento científico e pelas sugestões que tanto enriqueceram este trabalho. Também pela sua dedicação, ajuda nos momentos mais difíceis e, sobretudo, pela sua amizade e boa disposição.

À Patrícia, a minha Rainha da Investigação, que me apoiou, incondicionalmente, ao longo deste projeto. Para ti, as palavras serão sempre poucas para te agradecer tudo o que foi vivido ao longo deste ano. Foram dias de muita partilha, tanto a nível profissional, como pessoal. Obrigada por te dedicares a este projeto como se fosse teu! Obrigada por todas as resoluções dos problemas que me foram surgindo, pelas horas infindáveis de ajuda e de conselhos! Obrigada pela tua boa disposição e por fazeres com que muitos dos meus dias cinzentos passassem a ter a tua boa energia! Obrigada pelo teu carinho! Obrigada também por me ralhares, por me chamares à atenção quando devias, pelos choros, que me fizeram crescer tanto! Obrigada pelos risos e sorrisos! Sem dúvida que a aprendizagem contigo foi total!

Ao Augusto, o meu mais sincero Obrigada, por todo o teu infindável conhecimento científico, pela tua exigência, pela tua ajuda e apoio crucial neste projeto. És um exemplo, o teu profissionalismo é inquestionável!

Aos meus colegas de laboratório e amigos incríveis que quero para a vida toda, os meus "Milos" do coração, a Joana, o Joel, o João e o Pedro. Obrigada por me acompanharem desde o meu primeiro dia na Covilhã, por me deixarem ter a amizade que temos hoje. Este projeto é também, vosso, por todo o apoio e ajuda diária! Pela paciência nos momentos mais stressantes e pela força nestes últimos tempos. Obrigada!

Às minhas melhores amigas, Diana, Luciana e Mariana's, o meu obrigada por serem as amigas que sempre quis ter, pelo vosso apoio em todos os meus projetos, por estarem lá sempre que preciso. Mesmo longe, sempre presentes!

Ao Pedro, o meu profundo Obrigada! Obrigada por não teres desistido de mim, por me dedicares tanto do teu tempo, pela tua ajuda em superar o que surgia. Obrigada pela história tão bonita que conseguimos construir! Por seres o meu parceiro em tudo, mas principalmente, pelo teu carinho e pelo teu amor!

Por último, dirijo um especial agradecimento aos meus heróis, os meus Pais! Tudo o que sou devo-o a vós, que me transmitistes os melhores valores e educação. Obrigada por tudo, pela confiança que sempre depositastes em mim, pelo apoio e suporte incondicional, por permitirdes que todos os meus projetos se realizem e por me encorajardes a nunca desistir. Ao meu irmão Ricardo e à Andreia pelo incentivo nesta etapa tão importante da minha vida.

A força que tenho, é vossa. Amo-vos!

Resumo

O cancro do pulmão tem sido, desde há várias décadas, o tumor mais frequente do mundo, representando 13% dos novos casos de cancro anualmente em Portugal. A baixa eficiência dos tratamentos convencionais, devido à reduzida especificidade e acumulação de fármacos nos tumores, levou ao interesse em explorar novas estratégias terapêuticas. A terapia génica, aliada com a nanotecnologia, é uma das áreas mais extensas de investigação para o cancro do pulmão, em que o principal objetivo é desenvolver um tratamento seguro e eficiente, através da marcação específica e eliminação de células cancerígenas.

Os microRNAs (miRNAs) têm surgido com a possibilidade de serem usados como biofármacos para o tratamento de diversas doenças, incluindo cancro do pulmão. Os miRNAs são pequenos RNAs não codificantes que modulam, activamente, os processos fisiológicos das células como a apoptose, o controlo do ciclo e proliferação celular, reparação do DNA e metabolismo. A família do miR-29 (29a, 29b, 29c) possui complementaridade para as regiões 3'UTR das DNA metiltransferases (DNMT) 1, 3A e 3B, que são proteínas-chave envolvidas na metilação do DNA, frequentemente desreguladas no cancro do pulmão de não-pequenas células. Assim, tornou-se necessário investigar a relação do pre-miR-29 na regulação dos níveis das DNMTs, uma vez que permitem normalizar os padrões de metilação.

Neste trabalho, a produção do pre-miR-29 humano baseou-se na produção recombinante, utilizando o hospedeiro bacteriano *Escherichia coli* (*E. coli*) *DH5a*. Posteriormente, desenvolveu-se uma estratégia de purificação, baseada em cromatografia de afinidade, utilizando uma matriz de arginina superporosa, para purificar o pre-miR-29. Para a entrega do pre-miR-29 nas células cancerígenas e, para permitir alguma protecção da biomolécula, foi avaliada a possibilidade de encapsular o pre-miR-29 numa nanopartícula. Para isso, foram desenvolvidos e caracterizados sistemas de entrega não-virais, como sistemas poliméricos (poliPLEXOS). As formulações foram preparadas com polímeros biodegradáveis, Polietilenimina (PEI) e

Quitosano (CS), que demonstraram elevada eficiência de encapsulação, tamanhos pequenos e exibiram uma forte carga positiva na sua superfície. Além disso, a funcionalização destes sistemas de entrega com a lactoferrina (Lf), um ligando específico, permitiu melhorar o reconhecimento das partículas pelos receptores que se encontram na superfície apical das células epiteliais brônquicas.

Por fim, avaliou-se a actividade celular do pre-miR-29 recombinante na inibição da expressão de DNMT1, através da técnica de RT-qPCR. Os resultados indicaram que, o pre-miR-29 representa um produto biofarmacêutico promissor para a modulação terapêutica dos níveis de DNMT1 uma vez que, se obteve uma inibição da expressão proteica de cerca de 36% usando o poliplexo PEI-SA-Lf e 49% para o CS-SA-Lf. Esta regulação da DNMT I, poderá ser um indicador da possibilidade de restabelecer a expressão de genes supressores tumorais silenciados pela metilação, como o FHIT e WWOX e, assim, inibir a tumorigenicidade *in vitro*.

Palavras-chave: Cancro do Pulmão; Produção Recombinante; Pre-miR-29 humano; Silenciamento Génico; Cromatografia de Afinidade; Poliplexos.

Abstract

Lung cancer has been the most frequent tumor in worldwide for several decades and represents 13% of new cases of cancer annually in Portugal. The low efficiency of conventional treatments, due to the low specificity and accumulation of drugs in tumors has led to the development of new therapeutic strategies. The targeted gene therapy allied with nanotechnology is one of the most extensive area of lung cancer research, where the crucial aim is to develop safe and effective treatment through specific targeting and elimination of cancer cells.

The hypothesis that microRNAs (miRNAs) can be used as biopharmaceuticals has been emerging for treatment of incurable diseases, including lung cancer. MiRNAs are small noncoding RNAs which actively modulate cell physiological processes as apoptosis, cell cycle control, cell proliferation, DNA repair, and metabolism. The miR-29 family (29a, 29b, 29c) has complementarities to the 3'UTRs of DNA methyltransferase (DNMT) 1, 3A and 3B, which are key proteins involved in DNA methylation, frequently up-regulated in non-small-cell lung cancer and associated with poor prognosis. Thus, it is necessary to investigate the role of pre-miR-29 in regulation of DNMTs levels, which could normalize the aberrant patterns of methylation.

In this present work, the human pre-miR-29 production was based in recombinant production, using the bacterial host *Escherichia coli* (*E. coli*) *DH5a*. Afterwards, it was studied a purification strategy, based on affinity chromatography, using a superporous arginine matrix, to purify the pre-miR-29. For the delivery to lung cancer cells and to provide some protection to the target molecule, it was evaluated the possibility to encapsulate the pre-miR-29 into a nanoparticle. For this purpose, non-viral delivery systems, such as polymeric systems (polyplexes), were developed and characterized. The formulations were prepared with biodegradable polymers, namely polyethylenimine (PEI) and chitosan (CS), which demonstrated high loading capacity, small sizes and exhibited a strong positive charge on their surface. Further, the functionalization of these delivery systems with a specific ligand,

lactoferrin (Lf), was performed to improve the particle recognition by the receptors on the apical surface of bronchial epithelial cells.

Finally, the cellular activity of the recombinant pre-miR-29 at inducing translation inhibition of DNMT1 was evaluated using RT-qPCR. The results indicate that recombinant pre-miR-29 can represent a promising biopharmaceutical product for the therapeutic modulation of human DNMT1 levels, because it was achieved an inhibition of the protein expression of about 36% for the PEI-SA-Lf and 49% for CS-SA-Lf. This regulation of DNMT I, can also induce the re-establishment of methylation-silenced tumor suppressor genes expression, such as FHIT and WWOX, and thus inhibiting tumorigenicity *in vitro*.

Keywords

Recombinant Production; Human pre-miR-29; Gene silencing; Affinity Chromatography; Polyplexes; Lung cancer disease;

Table of Contents

Resumo	ix
Abstract	xi
List of Figures	xv
List of Tables	xvii
List of Abbreviations	xix
List of Scientific Publications	xxi
CHAPTER I - Introduction	1
1. RNA interference technology	1
1.1. Non-coding RNAs	1
1.2. MicroRNA biogenesis	4
1.3. MicroRNAs as therapeutic products	6
1.4. Sources of microRNAs	7
1.4.1. Chemical synthesis and <i>in vitro</i> transcription procedures	7
1.4.2. <i>In vivo</i> production and isolation of recombinant microRNAs	8
1.5. Purification of microRNA	9
1.5.1. Conventional strategies	10
1.5.2. Amino-acid-based Affinity Chromatographic strategies	11
1.5.2.1. New trends in Amino acid-based Affinity Chromatography	13
1.6. Nucleic acids delivery systems	14
1.6.1. Cationic polymeric delivery systems	15
1.6.2. Functionalization of gene delivery systems to target cancer cells	21
2. Lung Cancer disease	22
2.1. Etiology and pathogenesis	22
2.2. DNA methyltransferases in the development and progression of lung cancer	23
CHAPTER II - Materials and Methods	27
2.1. Materials	27
2.2. Methods	27
2.2.1. Pre-miRNA-29 biosynthesis and isolation	27
2.2.2. Superporous-based arginine immobilization	29
	xiii

2.2.3. Pre-miRNA-29 purification	29
2.2.4. Agarose electrophoresis	30
2.2.5. Polyacrylamide electrophoresis	30
2.2.6. Synthesis and characterization of PEI conjugated with Stearic Acid	30
2.2.7. Nuclear Magnetic Resonance (NMR) Spectroscopy	31
2.2.8. Conjugation of sRNA with PEI-SA and CS-SA complexes	31
2.2.9. Particle size and zeta potential measurements	32
2.2.10. Scanning electron microscopy (SEM)	33
2.2.11. Determination of the encapsulation efficiency	33
2.2.12. Functionalization of PEI-SA and CS-SA with Lactoferrin	34
2.2.13. Sodium dodecyl sulfate-polyacrylamide gel electrophoresis (SDS- PAGE)	34
2.2.14. H1299 cell culture	34
2.2.15. Transfection of H1299 cells with polyplexes (CS-SA-Lf/PEI-SA-Lf/pre-miR-29)	35
2.2.16 Expression of DNMT1 mRNA in H1299 cells by RT-qPCR	35
CHAPTER III - Results and Discussion	37
3.1. Recombinant pre-miR-29 production and isolation	37
3.2. Superporous matrix functionalization with arginine	39
3.2.1. Purification of pre-miR-29 with the superporous-arginine matrix	41
3.3. Synthesis and characterization of PEI-SA, CS-SA, CS-SA-Lf and PEI-SA-Lf complexes	46
3.3.1) ¹ H NMR analysis	47
3.3.2) Structural properties of PEI-SA and CS-SA complexes	49
3.4 SEM	58
3.5. Functionalization of PEI-SA and CS-SA with Lf	60
3.6. Preparation of PEI-SA-Lf-pre-miR-29b and CS-SA-Lf-pre-miR-29b	63
3.7. In vitro transfection and expression	63
3.7.1. Evaluation of DNMT1 protein knockdown induced by pre-miR-29-loaded complexes	63
CHAPTER IV - Conclusions and Future Perspectives	65
CHAPTER V - Bibliography	69

List of Figures

- Figure 1. Biogenesis of microRNAs [13]. 5
- Figure 2. Synthesis of PEI. A) Acid-Polymerization of Aziridine to yield bPEI; B) Ring-opening polymerization of 2-ethyl-2-oxazoline followed by hydrolysis to yield IPEI. 19
- Figure 3. Chitosan chemical structure. 20
- Figure 4. Regulation of miRNA expression by DNA methylation and its impact on lung tumorigenesis. 25
- Figure 5. Global process employed in this work for the recombinant biosynthesis and isolation of RNAs from *E. coli DH5a*. 37
- Figure 6. Representative growth curve of *E. coli DH5a* holding the pBHSR1-RM-pre-miR-29. 38
- Figure 7. A) Agarose gel electrophoresis of total RNA extraction containing recombinant pre-miR-29 from *E. coli DH5a*. The lanes 1 and 2 correspond to RNA samples obtained from two independent RNA extractions. B) Polyacrylamide electrophoresis of sRNA sample, with the mixture of RNA species (6S, pre-miR-29 and tRNA). 38
- Figure 8. Affinity purification strategy for recombinant RNA isolation with a superporous-arginine column. 40
- Figure 9. Chromatographic profiles of sRNA interaction with superporous matrices. A) Superporous matrix without arginine immobilized; B) Superporous matrix modified with the arginine ligands. 41
- Figure 10. A) Chromatographic profile of the pre-miR-29 purification from a sRNA mixture using the superporous arginine matrix. 42
- Figure 11. A) Chromatographic profile of the pre-miR-29 purification from a sRNA mixture using the superporous arginine matrix. 43
- Figure 12. A) Chromatographic profile of the pre-miR-29 purification from a sRNA mixture using the superporous arginine matrix. 44
- Figure 13. PEI ¹H NMR spectrum without SA. 47
- Figure 14. SA and the amino group of PEI in the presence of EDC, a carboxyl activating agent. 48

Figure 15. CS ¹ H NMR spectrum without SA.	48
Figure 16. SA and the amino group of CS in the presence of EDC, a carboxyl activating agent.	49
Figure 17. Agarose gel electrophoresis of sRNA/PEI polyplexes at various N/P ratios. The first lane of the gel corresponds to free sRNA.	50
Figure 18. Encapsulation efficiency of sRNA/PEI polyplexes at various N/P ratios.	51
Figure 19. Agarose gel electrophoresis of sRNA/CS polyplexes at various N/P ratios.	51
Figure 20. Encapsulation efficiency of the sRNA/CS polyplexes obtained from various N/P ratios.	52
Figure 21. A) Particle size for different N/P ratios of PEI (2kDa) conjugated with sRNA.	53
Figure 22. A) Zeta potential analysis for different N/P ratios of PEI (2kDa) conjugated with sRNA. B) Measurement of zeta potential distribution to confirm the defined charge of the particle.	55
Figure 23. A) Particle size for different N/P ratios of CS-MMW conjugated with sRNA.	56
Figure 24. Zeta potential analysis for different N/P ratios of CS-MMW conjugated with sRNA.	57
Figure 25. PEI-SA polyplexes obtained by simple complexation at pH 4.5 visualized by SEM.	58
Figure 26. CS-SA polyplexes obtained by simple complexation at pH 4.5 visualized by SEM.	59
Figure 27. SDS-PAGE of PEI-SA-Lf and CS-SA-Lf.	60
Figure 28. <i>In vitro</i> gene silencing effect of recombinant pre-miR-29b conjugated with PEI-SA-Lf and CS-SA-Lf on the DNMT1 mRNA levels, in H1299 cells normalized to GAPDH mRNA.	64

List of Tables

Table 1. General properties of ncRNA.	2
Table 2. Biological functions regulated by ncRNAs [13].	3
Table 3. Conventional agarose-based amino-acid affinity chromatographic matrices for recombinant pre-miR-29 purification.	12
Table 4. Main biological barriers in genetic material delivery.	15
Table 5. Advantages and Disadvantages of Non-viral vectors.	16
Table 6. Nanomaterials - Features of different types of nanoparticles.	17
Table 7. Main characteristics of polycations.	32
Table 8. Polyplexes characterization.	62

List of Abbreviations

3'UTR	3'-Untranslated Regions
5'UTR	5'-Untranslated Regions
Ago	Argonaute
<i>C. Elegans</i>	<i>Caenorhabditis elegans</i>
cDNA	Complementary DNA
CS	Chitosan
DGCR8	DiGeorge Syndrome Critical Region Gene 8
DNA	Deoxyribonucleic Acid
DNMT	DNA methyltransferases
dsRNA(s)	Double-stranded RNA(s)
<i>E. coli</i>	<i>Escherichia coli</i>
EE	Encapsulation Efficiency
EMA	<i>European Medicines Agency</i>
EMA	European Agency for the Evaluation of Medical Products
Exp-5	Exportin-5
FDA	Food and Drug Administration
gDNA	Genomic DNA
lncRNA(s)	Long Non-coding RNA(s)
miRISC	miRNA-Induced Silencing Complex
miRNA(s)/miR(s)	MicroRNA(s)
mRNA	Messenger RNA
NcRNA(s)	Non-coding RNA(s)
nt	Nucleotide
OD ₆₀₀	Optical Density at 600nm
PCR	Poly Chain Reaction
PEI	Polyethylenimine
PLGA	Poly(lactic-co-glycolic acid)
pDNA	Plasmid DNA

piRNAs	PIWI-Interacting RNA(s)
pre-miRNA(s)	Precursor MicroRNA(s)
pri-miRNA(s)	Primary MicroRNA(s)
<i>R. sulfidophilum</i>	<i>Rhodovulum sulfidophilum</i>
RISC	RNA-induced Silencing Complex
RNA	Ribonucleic Acid
RNAi	RNA Interference
RNA Pol II	RNA Polymerase II
RNA _t	Total RNA
RNase(s)	Ribonuclease(s)
rRNA(s)	Ribosomal RNA(s)
RT-qPCR	Quantitative Real Time PCR
SA	Stearic Acid
shRNA	Short Hairpin RNAs
siRNA(s)	Small Interfering RNA(s)
snRNA(s)	Small Nuclear RNA(s)
snoRNA(s)	Small Nucleolar RNA(s)
sRNA(s)	Small RNA(s)
SPE	Solid-phase extraction
tRNA(s)	Transfer RNA(s)
TSG(s)	Tumor Suppressor Gene(s)
WHO	World Health Organization

List of Scientific Publications

I. Smart micelleplexes as a new therapeutic approach for RNA delivery

P. Pereira, M. Barreira, J. A. Queiroz, F. Veiga, F. Sousa, A. Figueiras

Expert Opinion on Drug Delivery (2016)14: 353-371

Poster Communications

I. Pre-miR-29 as lung cancer therapeutics: Improving purity with ionic liquids and delivery with functionalized nanosystems

Maria Barreira, Patrícia Pereira, Augusto Pedro', Ana Figueiras, Fani Sousa

II Congress in Health Sciences Research: Towards Innovation and Entrepreneurship Trends in Biotechnology and Biomedical Applications, 17 to 20th May 2017, Covilhã, Portugal

II. Ionic-liquid aided affinity chromatographic purification of pre-miR-29 and targeted-delivery with nanoparticles for further application in lung cancer

Maria Barreira, Patrícia Pereira, Augusto Pedro', Ana Figueiras, Fani Sousa

XII Annual CICS-Ubi Symposium 2017. Covilhã, Portugal

CHAPTER I - Introduction






1. RNA interference technology

1.1. Non-coding RNAs

In 2006, Andrew Z. Fire and Craig C. Mello were awarded with the Nobel Prize in Physiology/Medicine for their discovery, RNA interference (RNAi), leading to a revolution in RNA understanding [1]. This discovery was remarkable, being recognized that RNA is not a simple intermediate in the information flux between DNA and proteins, but a versatile and dynamic molecule that controls numerous cellular processes essential to all living systems [2].

RNAi is defined as a well-conserved intracellular mechanism that allows the silencing/regulation of the gene expression by directing degradation or blocking the translation of its target messenger RNA (mRNA), through non-coding RNAs molecules (ncRNAs) action [3, 4] ncRNAs are a class of transcripts which, as the name implies, are not translated into proteins, but instead play important roles in diverse cellular functions [5]. According to their size, they can be classified into two major groups: small (<200 nucleotides in length) and long ncRNAs (from 200 nucleotides to approximately 100 kilobases) [5]. Within these large groups, the small ncRNAs are subdivided into regulatory RNAs, including microRNAs (miRNAs or miRs), small interfering RNAs (siRNAs), short hairpin RNA (shRNA) and Piwi-interacting RNAs (piRNAs), and, the structural RNAs, namely ribosomal RNA (rRNA), transfer RNA (tRNA), small nuclear RNA (snRNA) and small nucleolar RNA (snoRNA) that are involved in the spliceosomal and translational machinery (see Table 1)[3, 5, 6].

Table 1. General properties of ncRNA.

Class	Mean Size (bp)	Origin	Structure	Biogenesis	Action Mechanism	[Ref.]
miRNA	21-25	Endogenous	Double stranded 	Two-step cleavage of hairpin precursors by Drosha and Dicer	Induce translation repression or mRNA degradation	[6–8]
siRNA	19-25	Exogenous or Endogenous	Double Stranded 	Cleavage of long endogenous double strand RNAs by Dicer	Induce mRNA degradation	[6, 7, 9]
shRNA	19-29	Exogenous	Single Stranded 	Processed by Dicer to produce siRNA, transcribed by RNA polymerase III	Induce mRNA degradation	[9, 10]
piRNA	24-31	Endogenous	Single Stranded 	Transcribed from specific genomic loci in primary piRNAs that associate with the PIWI proteins	Can lead to the target RNA molecules degradation	[8, 10]
Long ncRNAs	200 to >100 Kb	Endogenous	Double Stranded 	Transcribed of primary long non-coding transcripts by RNA polymerase II into smaller non-coding RNAs	Induce translation repression or mRNA degradation	[6, 11, 12]

In the last decade, several studies showed that many of these small regulatory ncRNAs have important regulatory functions in a wide variety of physiological mechanisms (see Table 2), namely cell viability, cell cycle regulation, stem cell self-renewal, transposon activity control, cell proliferation and differentiation, heterochromatin formation and maintenance of cell integrity by gene silencing pathways [9].

Table 2. Biological functions regulated by ncRNAs [13].

Function	siRNAs	miRNAs	piRNAs
Protection of the cell/ genome against viruses	✓	✓	
mRNA deadenylation/ sequestration	✓	✓	
Heterochromatin Formation	✓	✓	✓
Genome Integrity and Stability	✓	✓	✓
Drug Resistance	✓	✓	✓
Developmental Robustness			✓
Evolution			✓
Transposon activity regulation			✓
Genome Reorganization			✓
Telomere Protection Complex			✓
Germ line development			✓
Epigenetic Regulation	✓	✓	
Chromatin Remodeling	✓	✓	
Histone and DNA methylation	✓	✓	
Protein synthesis inhibition	✓	✓	
RNA stability	✓	✓	
Biomarkers	✓	✓	
Maintenance of cell integrity	✓	✓	✓
Transcriptional inhibition (mRNA decay)	✓	✓	✓
Post-transcriptional RNA processing	✓	✓	✓

The regulatory ncRNAs play important roles in modulating various biological and cellular functions, and, therefore, present numerous clinical applications for treating a several number of human diseases caused by one or few genes, such as metabolic diseases, cardiovascular diseases, hypertension and stroke, immune dysfunction and autoimmune disorders, neurodegenerative and psychiatric diseases and distinct types of cancers [6, 7, 14].

RNAi-based drugs present attractive characteristics over traditional pharmaceutical drugs, such as its simplicity, high specificity, high degree of safety, high efficacy, ability to induce a potent knockdown of the targeted genes and, in addition, the ability to promote a long-lasting therapeutic effect, which can last from days up to weeks [2, 15, 16]. In this way, as low doses are required for ncRNAs therapeutics, along with a possible reduction of undesirable adverse effects, it should also be expected a decrease in the expenses of these medical treatments [2].

1.2. MicroRNA biogenesis

The discovery of miRNAs functions and their therapeutic potential has been one of the most fascinating breakthroughs of recent times and, actually, they represent the most extensively studied class of ncRNAs due to their great potential for therapeutic knockdown of disease-causing genes [17]. At present, 2588 mature miRNAs are currently annotated in the human genome (<http://www.mirbase.org>, miRBase release 21, June 2017). MiRNAs are small, endogenous, evolutionarily conserved molecules and are directly involved in the regulation of gene expression at the post-transcriptional level via base-pairing interactions between the 5' end of the miRNA and the 3'UTR of their target mRNA, which, depending on the degree of sequence complementarity, can result in mRNA translational repression or degradation [6, 18].

The post-transcriptional regulation mechanism involving miRNAs occurs through a sequential process, as outlined in Figure1.

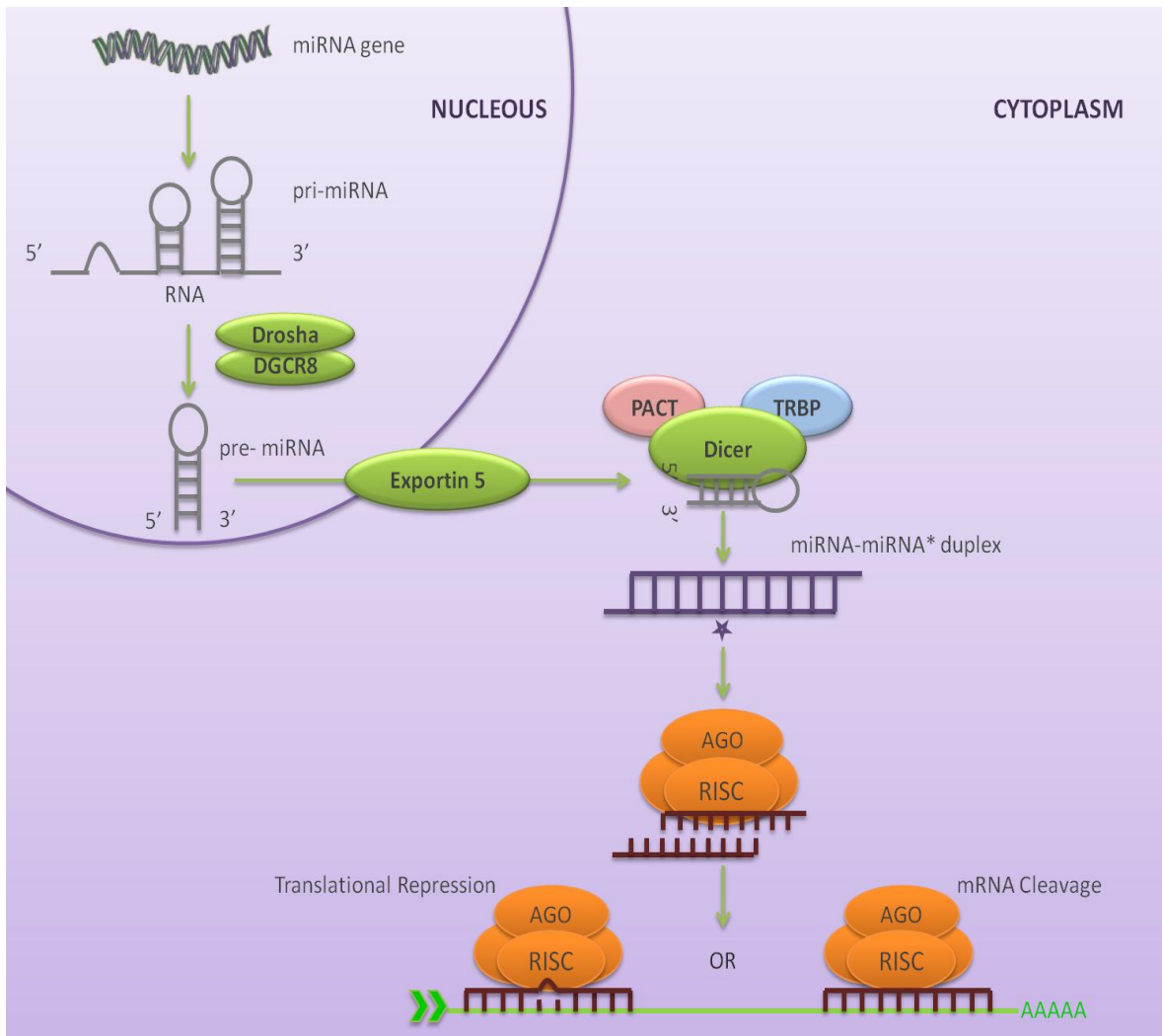


Figure 1. Biogenesis of microRNAs [13].

The miRNA biogenesis begins in the nucleus, with the long primary miRNA transcripts (pri-miRNAs, containing more than 100 nucleotides and a characteristic loop-stem morphology), which contains the mature miRNA sequence, being produced by RNA polymerase II [18]. Then, these pri-miRNAs transcripts are recognized and cleaved by a complex containing the RNase III, Drosha and DiGeorge syndrome critical region gene 8 (DGCR8), leading, subsequently, to a long hairpin precursor of miRNA (pre-miRNA, with 70–110 nucleotides) [19]. Subsequently, the pre-miRNA is transported to the cytoplasm to be processed, through Exportin-5, a nuclear transport complex, and its loop is removed by a complex that contains the enzyme Dicer (ribonuclease III), TRBP (Tar RNA-binding protein) and PACT (protein

kinase R-activating protein). After that, the resulting product is a mature double strand miRNA (miRNA-miRNA*) with variable length, between 19–25 nucleotides and is unwound in two strands: miRNA is the antisense strand (or guide strand) and miRNA* is the sense strand (or passenger strand) [18].

Then, in the RISC complex, mature miRNAs are associated with the Argonaute (Ago) proteins, specifically Ago1 and Ago2. The antisense, miRNA strand is loaded into RISC complex, to form the miRNA silencing complex (miRISC) that will bind to the 3' untranslated regions (3'UTR) of the target mRNA, whereas the sense chain (miRNA*) is stamped and released for degradation [20]. When the miRNA-mRNA base-pairing complementarity is perfect, occurs the degradation of mRNA transcripts; otherwise, if imperfect base pairing prevails, it arises a translational repression by blocking mRNA translation [18, 21].

1.3. MicroRNAs as therapeutic products

Nowadays, miRNA-based therapy has emerged as a promising strategy for the treatment of different human diseases. As mentioned above, they have been implicated as a master regulators of a variety of physiological and cellular processes [20]. For this reason, the identification of deregulated miRNAs and their responsive targets in different pathological states may provide not only potential biomarkers for diagnostic purposes, but also new therapeutic agents [22]. Depending on their targets in different tissues and cell types, miRNAs can be considered tumor suppressors or tumor promoters [23].

Recently, there is overwhelming evidence of abnormal miR-29 family expression profiles in malignant cell and all exert anti-tumor functions, being involved in the regulation of cell proliferation, differentiation, and apoptosis. Downregulation of miR-29 family members has been correlated with many types of cancer including leukemia [24] [25], melanoma [26], liver [27], colon [28], cervical [29] and lung cancers [30].

The miR-29 family is among the most studied miRNAs, and it includes miR-29a, miR-29b, and miR-29c, which differ in only two or three nucleotides. miR-29b is

more often expressed and is found at two genomic loci [31]. However, although these similarities, the isoforms of miRNA-29 may execute distinct functions. As a regulator, the miR-29 family is involved in the expression of several genes. For example, in Alzheimer disease (AD), miR-29 is potentially involved in the regulation of amyloid precursor protein (APP) and BACE1 protein expression. The interconnection between miR-29 and AD, is explained by the decreased levels of miR-29 that is correlated with increased levels of BACE1 expression [32]. In Acute Myeloid Leukemia (AML), previous studies showed that miR-29a and miR-29b could function as tumor suppressors in leukemogenesis, by targeting protein kinase B2 (AKT2) and cyclin D2 (CCND2), two key signaling molecules [33].

1.4. Sources of microRNAs

The discovery of RNA interference together with the rapidly growing of miRNAs therapeutic applications, underline the importance of developing strategies to obtain high levels of miRNAs, either for therapeutics or for structural and functional studies. Contrary to other biomolecules such as DNA and proteins for which well-established protocols allow to obtain high yields with high homogeneity, working with RNA poses additional challenges. Indeed, RNA is more prone to degradation by nucleases than DNA, what results in greater requirements for clean and controlled environment; also, the technical options to produce large amounts of RNA are more limited. Therefore, independently of the RNA source, special precautions have to be taken, mainly focused on inactivating nucleases and to prevent RNA hydrolysis [34].

1.4.1. Chemical synthesis and *in vitro* transcription procedures

Most of the miRNAs used in the development of new therapeutics are obtained by two different ways, namely by chemical synthesis (via phosphoramidite solid phase chemical chemistry) [35], or using enzymatic methods (*in vitro* transcription) [36]. Aiming the reduction of RNA instability as well as the control of

degradation by cellular ribonucleases, these processes usually introduce unnatural modifications (chemical modifications) in the synthesized RNA. The chemical synthesis of RNA presents some disadvantages, namely the low yield and high cost of the process that proportionally increases with the length of the oligonucleotide to be synthesized. Moreover, there is some uncertainty whether the modified RNA will remain stable, and able to maintain its biological activity. On the other hand, the enzymatic methods are generally less efficient because it is necessary to transcribe the DNA to RNA precursors, and this is dependent on the action of RNA polymerases [37]. In order to complete these processes it is also necessary to carry out purification protocols to remove the contaminants derived from the synthesis process, namely linearized plasmid DNA template, enzymes, free nucleotides, salts or buffers, short aberrant transcripts, failure in the sequences, among others [38]. The presence of these impurities leads to disadvantages for subsequent clinical applications, since they may lead to non-targeted gene silencing, what is commonly associated to a decrease in therapeutic effectiveness [38].

1.4.2. *In vivo* production and isolation of recombinant microRNAs

Considering the importance of miRNAs as new biopharmaceuticals with clinical application, the methodologies for their manufacturing should be improved for an easy production, while maintaining the stability and quality of the biomolecule. Moreover, this process should be economic and efficient for the large-scale production of miRNAs. In this way, the *in vivo* expression of recombinant RNA molecules using microbial hosts such as bacteria, might be the most promising strategy, since it can reduce the costs, but keeping a highly efficient process [39]. The recombinant expression of RNAs has been accomplished using different bacteria, mainly *Escherichia coli* (*E. coli*) [39, 40] and *Rhodovulum sulfidophilum* (*R. sulfidophilum*) [41, 42].

The methodologies employed for production and recovery of RNA using these hosts can differ. In particular, *R. sulfidophilum* presents the ability to differentially secrete the RNAs to the extracellular medium in the absence of ribonucleases, thus

simplifying their recovery devoid of main bacterial associated impurities [41, 43, 44]. In *E. coli*, after the fermentation step, it is necessary to perform cell lysis to recover the intracellular RNA, what can be responsible for the release of endotoxins, and consequently, lead to the contamination of the RNA sample [45, 46]. However, *E. coli* growth kinetics is much faster than for example *R. sulfidophilum*, allowing to perform a fermentation experiment in just one day (8 hours), compared with a 4-day period required by *R. sulfidophilum* [47].

When the target recombinant RNA is produced intracellularly, it is necessary to proceed to cell lysis and RNA isolation, what is traditionally achieved with the guanidinium thiocyanate-phenol-chloroform extraction. This method consists in the disruption of cells using a solution composed by guanidinium thiocyanate, phenol and chloroform, followed by precipitation [48]. The use of this procedure is controversial since it involves the use of denaturing agents (guanidinium thiocyanate and β -mercaptoethanol) and organic solvents (alcohols), which may compromise the success of several RNA based-procedures in clinical research [48]. However, this process is still the most widely used for isolating total RNA from biological samples of different sources, and it delivers high yields of RNA, very rapidly, retrieving small and large, low-abundance and high-abundance RNA isoforms. Throughout the extraction process, the aim is to maximize the RNA recovery with high quality, integrity, stability and biological activity, and, simultaneously, remove some contaminants and impurities, such as genomic DNA, sRNAs, proteins, endotoxins, salts, denaturing agents and organic solvents.

1.5. Purification of microRNA

In the past few years, different strategies and methods have been described for RNA purification, either for chemically synthesized RNAs or for RNAs derived from biological sources. In general, purification protocols used for RNA isolation have a number of common requirements, due to the high risk of RNA degradation during the procedure. So, the major interest is not only to produce high quantities of the final RNA product, but also to assure its quality, stability, integrity, biological activity,

and purity, fulfilling the requirements of regulatory agencies, such as FDA, European Agency for the Evaluation of Medical Products (EMA), or World Health Organization (WHO) [38].

1.5.1. Conventional strategies

RNA purification can be achieved using methods like preparative denaturing polyacrylamide gel electrophoresis and different chromatographic strategies, such as reversed-phase ion pair liquid chromatography, anion exchange and size exclusion chromatography, that can be applied as isolated or integrated steps [49, 50].

These purification methods can be efficient for RNA recovery with high resolution, however they require time-consuming preparatory steps and are expensive on large scale. Another disadvantage comes from the fact that different contaminants, such as acrylamide, lithium metal, ion-pairing agents and organic solvents, involved in these processes induce structural modifications on RNA, thus leading to its degradation [49, 51, 52]. The RNA obtained using these strategies may require treatments to be suitable for clinical application, which spoil the stability and the biological activity of the target RNAs. Thus, one of the most important challenges in the development of a purification strategy, arises from the need to obtain the target RNA with high purity and recovery yields, but equally important is to guarantee the maintenance of the RNA biologically active form, to comply with the requirements from the regulatory agencies.

1.5.2. Amino-acid-based Affinity Chromatographic strategies

The growing interest on the development of novel RNA-based therapeutic approaches demands for new and improved manufacturing strategies, for which highly selective and robust protocols should be available, capable of maintaining the structural integrity and biological activity of the target RNA. In the pursue of this aim, affinity chromatography [13] has gain much attention, since it represents a powerful technique for nucleic acids purification. In affinity chromatography, biomolecules are separated from each other based on a reversible interaction between the target biomolecule and its specific ligand, which is coupled to a chromatographic matrix. Moreover, the specific interactions occurring between the ligand and the target molecule may include electrostatic interactions, hydrophobic interactions, van der Waals forces and/or hydrogen bonding, resulting in high selectivity and high resolution [53].

A promising approach in affinity chromatography is the use of amino acids as specific ligands, which mimic the biological and reversible interactions that occur at cellular level between proteins and nucleic acids [54, 55]. This technique allows the purification of nucleic acids with high selectivity, specificity, efficiency and makes this methodology a robust process because of the use of stable and natural small molecular ligands. The selectivity is explained by the biological or chemical structure recognition, which favors the specific interactions [56]. Herewith, the binding/elution conditions, such as the temperature, pH and buffer composition (type of salt, ionic strength or presence of competitive agents), can be adjusted and optimized, aiming to maximize the purity and recovery of RNA [53]. In fact, amino-acid affinity chromatography strategies were already reported for the purification of different RNAs [38, 55, 57, 58], including the pre-miR-29, as depicted in Table 3 [59, 60].

Table 3. Conventional agarose-based amino-acid affinity chromatographic matrices for recombinant pre-miR-29 purification.

Chromatography Ligands	Elution Strategy	Observations	[Refs.]
O-Phospho-L-Tyrosine	<ul style="list-style-type: none"> - 3 stepwise decreasing gradient of ammonium sulfate - 2M (NH₄)₂SO₄ in 10mM Tris-HCl, pH 8.0; 	Low yield; <ul style="list-style-type: none"> • High salt concentration; High cost; Environmental impact;	[59, 61]
L-Lysine	<ul style="list-style-type: none"> - 1 stepwise gradient of ammonium sulfate - 2M (NH₄)₂SO₄ in 10mM Tris-HCl, pH 8.0; • - Linear gradient of sodium chloride; 	Salt concentration;	[62, 63]
L-Arginine	<ul style="list-style-type: none"> • - Increasing sodium chloride gradient - 360mM NaCl, pH 8.0; - Competition chromatography-elution buffer supplemented with arginine; - Decreasing ammonium sulfate ((NH₄)₂SO₄), between 2.4M and 0M in 10 mM Tris-HCl buffer, pH 8.0; 	High selectivity; High efficiency;	[58, 60]

These amino acid ligands described above showed high selectivity, however a faster and more robust purification method is required due to the structural characteristics of the RNA molecule, including its stability.

In general, using these strategies, it was verified that the separation is very fast, which allows to obtain a good yield of RNA with minimal degradation due to the shorter contact time with the chromatographic matrix; also, the analysis times are short while high reproducibility was obtained. Moreover, additional advantages include the efficient elimination of endotoxins, proteins and single/double-stranded RNAs, under non-denaturing conditions, and the possibility to easily adapt the method to any molecular weight RNA [46].

1.5.2.1. New trends in Amino acid-based Affinity Chromatography

As mentioned above, the affinity chromatography matrices with amino acids ligands immobilized in agarose supports showed high selectivity for pre-miR-29 purification, although some implications in RNA stability must be considered. Indeed, these columns have certain limitations, namely the low mass transfer, gel compressibility and poor pore diffusion leading to high pressure drops and low flow rates application, that leads to a more expensive process [64].

Accordingly, monoliths arise as an alternative support to conventional columns, capable of improving the efficiency of the purification process already established [64, 65]. They have been investigated for the separation of large biomolecules and hold structural properties that make them a promising strategy for RNA purification. These supports exhibit high binding capacity, high external porosity, excellent mass transfer properties and a huge quantity of accessible binding sites. Beyond that, monoliths concede the application of higher flow rates, fast separations, short analysis times and purification with high reproducibility either at small or large scales [65, 66]. In an attempt to combine the advantages of monoliths with the selectivity provided by amino acids-based affinity chromatography, an agmatine monolith was also employed for the purification of pre-miR-29. This monolithic support represents an advantageous alternative to conventional supports due to fast separations and consequent short contact time, ensuring structural stability of the target molecule. Moreover, the manipulation of the type and salt concentration and pH in the loading buffer allows the establishment of different interactions and

consequently the implementation of different elution strategies. The amino acid ligands will allow to obtain the pre-miR-29 with high degree of purity and good integrity due the fast separation and consequent short contact time with the support. Nevertheless, these supports still have a high cost [67].

Another breakthrough in RNA purification protocols may come from the use of superporous matrices. As the name implies, the superporous matrix contains a network of large through-pores that allows intraparticle mass transport by molecular convection, improving the effect of mass transfer resistance resulting from the mobile phase stagnated inside the pores. This matrix has large connecting flow pores with sizes in the range of 1/4 to 1/20 of the overall particle diameter (particle average size 106–180 nm), which supply the high binding capacity [64].

Some studies comparing superporous and non-superporous supports revealed that the superporous particles allowed an improved separation, high purification and recovery, as well as flow velocities five times higher than it was possible for non-superporous particles [68]. This superporous technology was firstly applied to agarose particles to purify proteins based in ion-exchange, affinity and hydrophobic chromatography, but the application in nucleic acids purification, namely for RNA, can be a promising strategy.

1.6. Nucleic acids delivery systems

The therapeutic application of miRNAs is clearly promising due to its simplicity, safety profile and easy manufacturing and, specifically, due to its ability for silencing gene expression [69, 70]. Along the years, in DDS (Drug Delivery System) development, different formulations have been studied with the aim to find new and efficient carriers for drugs and genetic material. However, the major challenge of miRNAs-based therapeutics for clinical applications is still the finding of a way of delivering these molecules to target cells or specific tissues without modifying their function, while preventing side effects [71]. Naked miRNAs are highly susceptible due to their rapid degradation by serum nucleases, and also because they can be accumulated by kidneys and rapidly eliminated in urine. Therefore, they present a

short life-time in the circulatory system, because their size is smaller than the size for glomerular filtration, resulting in a minimization of the therapeutic effect [72]. The intracellular barriers, such as inefficient cellular uptake and intracellular processing of endosome-targeted RNAs (escape from the endosome, vector unpacking and processing by the RNAi machinery) need to be surpassed before the therapeutic genetic material arrives to the cytoplasm, allowing an improvement on miRNA pharmacokinetic and pharmacodynamic properties [73].

Table 4. Main biological barriers in genetic material delivery.

Biological Barriers	
Extracellular Barriers	Intracellular Barriers
<ul style="list-style-type: none"> • Lipid bilayer membrane; • Blood components and opsonization; • Endothelial barriers (blood brain barrier, respiratory mucus). 	<ul style="list-style-type: none"> • Cell uptake; • Endosomal escape; • Intracellular trafficking; • Intracellular transport machinery; • Nuclear delivery.

So, it is necessary to develop an appropriate carrier system that can improve transport and delivery of RNAs to the cytoplasm of target cells, displaying reduced cytotoxicity and immunogenicity, protecting RNAs from serum nucleases, increasing the retention time of RNAs in the circulatory system and maintaining their stability under physiological conditions.

1.6.1. Cationic polymeric delivery systems

Gene delivery systems can be divided in viral vectors and non-viral vectors and they have been applied in different gene therapy strategies. Initially, viral vectors, were used by the researchers, because they exhibited high efficiency in genetic

material distribution, both *in vitro* and *in vivo*, allowing their cellular uptake and intracellular trafficking and enabling the expression of genes in the long term. More recently, with the identification of safety and immunogenicity problems associated with viral vectors, the focus has changed to the non-viral gene delivery approaches [74, 75].

Table 5. Advantages and Disadvantages of Non-viral vectors.

Non-Viral Vectors	
Advantages	Disadvantages
<ul style="list-style-type: none"> • Manufacture and quality control relatively simple; • Good storage characteristics; • Low immunogenicity; • Good safety profile; • Efficient transfection <i>ex-vivo</i>; • Delivery to any somatic cell; • Non-infectious; • No limit on size of genetic material. 	<ul style="list-style-type: none"> • Short duration of expression; • Repeated administrations required; • Inefficient transfection <i>in vivo</i>.

A new generation of nanomedicines has emerged, which uses novel self-assembled nanomaterials, including polymer-RNA complexes (“polyplexes”), liposomes, lipoplexes, lipid-based delivery systems, polymer micelles, pluronic block copolymers, cyclodextrins, nanogels, and other nanoscale sized materials for medical use [76–78].

Table 6. Nanomaterials - Features of different types of nanoparticles.

Nanomaterials		
Types of nanoparticles	Unique features	[Ref.]
Cationic polymer complexes	Oligonucleotides form complexes with cationic polymers such as PEI and modified polymers. Complexes are rapidly and easily prepared.	[79]
Polymeric micelles	The micelles are formed by the self-assembly of block copolymers via electrostatic interactions. The inherent and modifiable properties of micelles are suitable for gene delivery.	[80]
Dendrimers	3D macromolecules consist of a central core from which the highly branched polymer chains grow in symmetric structures. The properties of dendrimers can be controlled by varying the number of generations.	[81]
Solid Polymeric nanoparticles	Nanoparticles are formed by biodegradable polymers in different forms such as hollow or porous structures. Solid polymeric particles show high stability and controllable release of loaded drugs.	[82]
Liposomes	The most commonly used nanoparticles in gene delivery for lung cancer research. The lipid bilayers of liposomes provide high biocompatibility and allow efficient cellular uptake.	[83]

Pluronic block copolymers	<p>Pluronic block copolymers consist of hydrophilic ethylene oxide (EO) and hydrophobic propylene oxide (PO) blocks arranged in a basic A-B-A structure: EO_x-PO_y-EO_x.</p> <p>They are versatile molecules that can be used as structural elements in novel self-assembling gene delivery systems.</p>	[84]
Solid lipid nanoparticles	<p>Solid lipid nanoparticles (SLNs) is consisted of solid lipid core matrix that are enclosed and stabilized by a lipid monolayer on surface.</p> <p>Solid lipid particles show not only high stability as polymeric nanoparticles but also have the high affinity to cellular membrane as the liposomes.</p>	[85]
Metal-based nanoparticle systems	<p>Multifunctional metal-based nanoparticle systems can be used in therapeutic and diagnostic applications.</p> <p>Metal-based nanoparticles are usually coated or conjugated with polymers and lipids (also encapsulated in micelles or liposomes) for gene delivery purpose.</p>	[86]

These vehicles offer many advantages over the viral vectors, thus allowing the safe accumulation of RNA therapeutics in the site of interest, enhancing intracellular delivery and early endosomal escape, with high biocompatibility, low cytotoxicity, prolonged expression and enabling repeated administrations without significant immune response. Furthermore, they present a low production cost, high flexibility and easy quality control and the large-scale production is facilitated because it is possible to design the carriers with defined structure and chemical properties. As disadvantages, these systems present a reduced transfection efficiency, poor oral

bioavailability and instability in circulation [73, 75]. To overcome these limitations, some strategies have been applied, such as the use of polymers, namely polyethylenimine (PEI), chitosan (CS), polyethylene glycol (PEG), polylysine, poly(lactic-co-glycolic acid) (PLGA). Actually, one major approach in non-viral gene therapy is based on 'polyplexes', complexes formed by mixing nucleic acids with synthetic or natural polycations.

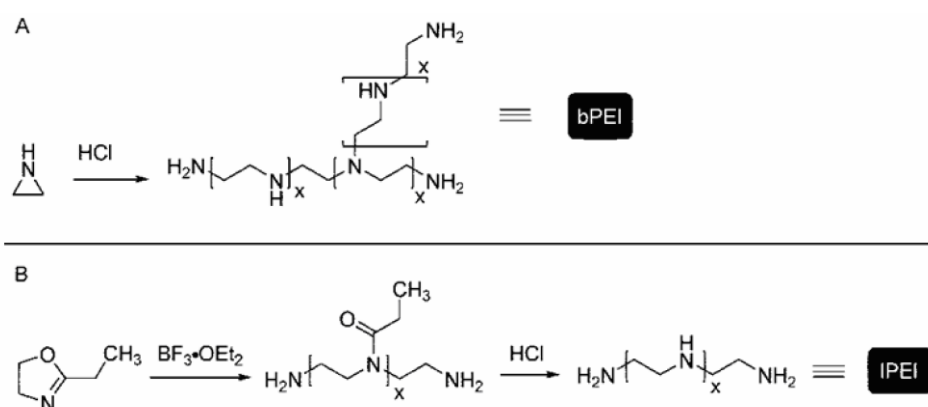


Figure 2. Synthesis of PEI. **A)** Acid-Polymerization of Aziridine to yield bPEI; **B)** Ring-opening polymerization of 2-ethyl-2-oxazoline followed by hydrolysis to yield IPEI.

Polyplexes are formed spontaneously as a result of electrostatic interactions between the positively charged groups of the polycation, and the negatively charged phosphate groups of the nucleic acids [87]. Regardless of the diversity of materials for synthesis of nanoparticulated systems, PEI and CS nanocarriers have been gaining a huge interest as non-viral gene delivery systems, mainly due to its unique properties. PEI is a cationic polymer that have linear and branched structures (Figure 2) [87, 88]. Branched PEI (bPEI) and linear PEI (IPEI) can both be used effectively for gene delivery. L-PEI is generally preferred for *in vivo* applications because of its low toxicity profile, however B-PEI contains primary, secondary, and tertiary amino groups in a 1:2:1 ratio [89]. The higher percentage of primary amines which is more suitable for modifications, they are mainly responsible for high degree of RNA binding, but also

contribute to toxicity during the transfection. Contrary, the secondary and tertiary amines provide good buffering capacity to the system.

The abundant presence of free amino groups makes PEI an attractive polymer for conjugation of various ligands to improve the transfection efficiency or targeted gene delivery. Due to its cationic charge density potential, it can form stable complexes with negatively charged (nucleic acids) through electrostatic interactions and bind to anionic cell surface residues to internalize into cells through endocytosis. In general, PEI has potential as a carrier, due to its superior transfection efficiency, which facilitate endosomal escape after entering the cells as it acts as a "proton sponge" during acidification of the endosome [90, 91]. Other properties, namely its ability to encapsulate large amounts of drug, high stability, biocompatibility, biodegradability, low cytotoxicity and immunogenicity, and reduced side effects make this polymer a greater alternative to improve gene delivery.

Additionally, CS is one of the most widely used cationic polymers for nucleic acids delivery with wide applications in pharmaceutical industry [100]. The main characteristic of CS, as a gene delivery vehicle is its cationic nature due to the primary amine groups present in its backbone (Figure 3).

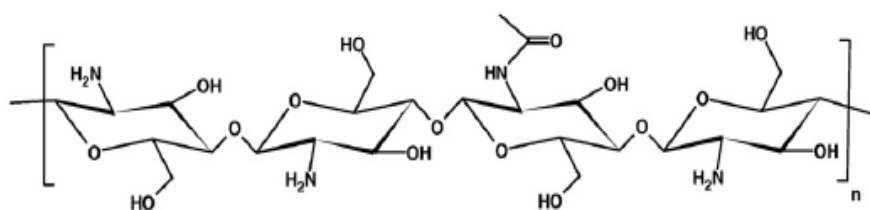


Figure 3. Chitosan chemical structure.

Protonation of the CS amine groups occurs at a pH below its pKa value of 6.5, however it is insoluble at neutral and alkaline pH values but soluble in an acidic medium, which greatly limits its further biomedical applications. It is also considered to be a good candidate for gene delivery, since it has beneficial qualities such as low toxicity, low immunogenicity, non inflammatory, excellent biodegradability,

biocompatibility [93, 94]. The strong protonation of amines enhances the electrostatic interaction between CS and nucleic acids to form complexes of nanoscale dimensions, allowing the transport across cellular membranes and subsequent endocytosis into cells [95].

Further, the polymer's surface functionality also plays an important role in conjugating ligands for therapeutic targeting into cancer cells. The specific delivery into cancer cells is an important strategy to improve therapeutic efficacy and reduce toxicity in normal tissues [91, 96].

1.6.2. Functionalization of gene delivery systems to target cancer cells

Nanocarriers are extremely important for the therapeutic delivery of RNAs, and they can be coated with high affinity ligands for tumor specific receptors, for a sustained release, with the aim to protect the miRNA release before achieving the target. This can be achieved through the surface modification of delivery systems with a ligand, such as a transferrin (Tf), lactoferrin (Lf), stearic acid (SA), targeting to the receptor. The stearic acid ligand facilitates the interaction with the specific molecules expressed in lung cancer cells, improving the particle selectivity, which leads to decreased side effects, and still increasing the passive targeting effect and the circulation time [97]. In this study, the conjugation of Lf and SA in the surface of the polyplexes (CS or PEI), will allow the specific binding of the nanosystem to the surface of bronchial epithelial cells [98].

To be an effective therapy for cancer, it is necessary to achieve two important points, the miRNA nano-carrier size should be suitable to enable the entrance into the tumor tissue, through the passage of the biological barriers, without losing the characteristics nor decreasing the RNA activity [73]. Then, after reaching the tumor tissue, the miRNA must be released through a controlled mechanism, to eliminate selectively the tumor cells without affecting healthy cells. This mechanism occurs immediately after the transport of these carriers into the endocytic vesicles, initially, where the pH drops to 6 followed by trafficking to late endosomes, which are acidified to pH 5-6. In these vesicles, it is prevented the subsequent degradation of

RNA by lysosomes. Then, they need to be released, and through the influx of chloride counter ions it is created an osmotic pressure inside the endosomes which leads to the release of the content trapped therein [71].

These two basic strategies are also associated with improvements in patient survival and quality of life by increasing the intracellular concentration of drugs and reducing dose-limiting toxicities simultaneously. These vehicles should be characterized regarding their safety, specificity and efficiency in gene transfer; magnitude and duration of expression; immunogenicity and manufacturing process [71].

2. Lung Cancer disease

2.1. Etiology and pathogenesis

Cancer is one of the diseases with the highest prevalence worldwide, being the second leading cause of death in developed countries. This complex disease includes several pathologies that can affect the normal growth and behavior of cells, which subsequently invade and metastasize to healthy tissues.

Lung cancer is the most preponderant form of cancer and it affects a large number of persons, in Portugal, represents 13% of new cases of cancer annually [99]. Lung cancer is classified in two types: small cell lung cancer (about 13%) and non small cell lung cancer (NSCLC) (about 87% of all lung cancers) [99]. Although there are new therapeutic regimens and new drugs, the prognosis for lung cancer patients has not significantly changed in the last 20 years. The main therapy for NSCLC is surgery in combination with chemotherapeutic agents, but a large fraction of patients cannot attain a regression in the disease, due to the poor therapeutic efficiency, non-specific interactions, and toxicity to normal tissues of this therapeutic approach.

For this reason, the innovation and development of novel therapeutic strategies is critical and essential for the treatment of this worrisome disease that affects a large number of people. The identification of new mutations and genetic rearrangements in approximately 50–60% of NSCLC has led to a change in the

treatment of lung cancer patients, by identifying subgroups of patients characterized by different molecular profiles. More than half of the 200,000 cases were diagnosed in former smokers because more than 3,000 chemicals have been identified and quantitated in tobacco smoke, many of which have been shown to directly or indirectly (e.g., through oxidative stress) generate a wide spectrum of DNA lesions. The most frequent DNA damage consists on bulky chemical base adducts; methylated bases; and a variety of oxidative lesions, and if unrepaired, many of these lesions cause lack of nucleotides incorporation or block synthesis by replicative DNA polymerases [100]. These alterations can lead to genetic changes ranging from substitution mutations to large-scale chromosomal aberrations and epigenetic alterations which are manifested in malignant tumors. Epigenetic modifications that also arise in response to DNA damage, and through their diversity of effects on the regulation of the gene expression, have a crucial role in cellular selection, leading to a growth advantage for the tumor cells [101]. These modifications, control the properties of a tumor cell, since they are involved in enhanced proliferation, growth suppressor evasion, antiapoptosis, replicative immortality, angiogenesis, inflammation, altered metabolism, genomic stability, and metastasis signaling [102].

In this way, specific alterations in DNA methylation patterns are hallmarks of human diseases and therefore could represent specific targets for treatment.

2.2. DNA methyltransferases in the development and progression of lung cancer

MiRNAs are reported to play an important role in post transcriptional silencing of target mRNAs involved in various human cancers. In lung cancer tissue, the miR-29 family (29a, 29b, and 29c) expression is associated to different levels of DNA methyltransferases DNMT1 and DNMT-3A/B, important enzymes for DNA methylation that are frequently upregulated. The role of miR-29 in the epigenetic normalization of non-small cell lung cancer (NSCLC), provided a rationale for the development of miRNA-based therapeutic interventions for the treatment of lung cancer [103].

The miRNA therapy is introduced in two different ways: one is, that miRNAs play an essential role in lung development and their expression levels are deregulated in lung cancer cells compared to normal tissues and, the second one, is that several studies demonstrated that modulation of miRNA expression, both *in vitro* and *in vivo*, can modify the cancer phenotype. The hypermethylation have aided to a paradigm change in molecular diagnosis and treatment of lung cancer, since it is responsible for the silencing of tumor suppressor genes (TSGs) involved in lung carcinogenesis, such as CDKN2A [104], CDH13 [104], FHIT [105], WWOX [105], CDH1 [106], and RASSF1A [107] [108].

Some studies suggest that the loss or mutations on the genes encoding miRNAs, such as variations in the number of copies and the hypermethylation-mediated silencing of the miRNA-encoding genes, contribute to the deregulation in the miRNA expression. Aberrant cytosine methylation and chromatin remodeling within CpG islands mediate epigenetic silencing of genes and microRNAs during tumor development. This methylation is mediated by a family of DNA methyltransferase enzymes (DNMT1, DNMT3A and DNMT3B) that transfer a methyl group from S-adenosyl-L-methionine to cytosines in CpG dinucleotides [100]. The elevated DNMT1 expression has been shown to predict a poorer prognosis, and elevated expression of both DNMT1 and DNMT3B have been shown to be correlated with hypermethylation of TSG promoters.

In lung cancer case, the expression of miR-29 families, replace the natural patterns of DNA methylation, inducing restatement of tumor suppressor genes, such as FHIT and WWOX, which was previously silenced by methylation, therefore inhibiting the tumorigenicity (Figure 4).

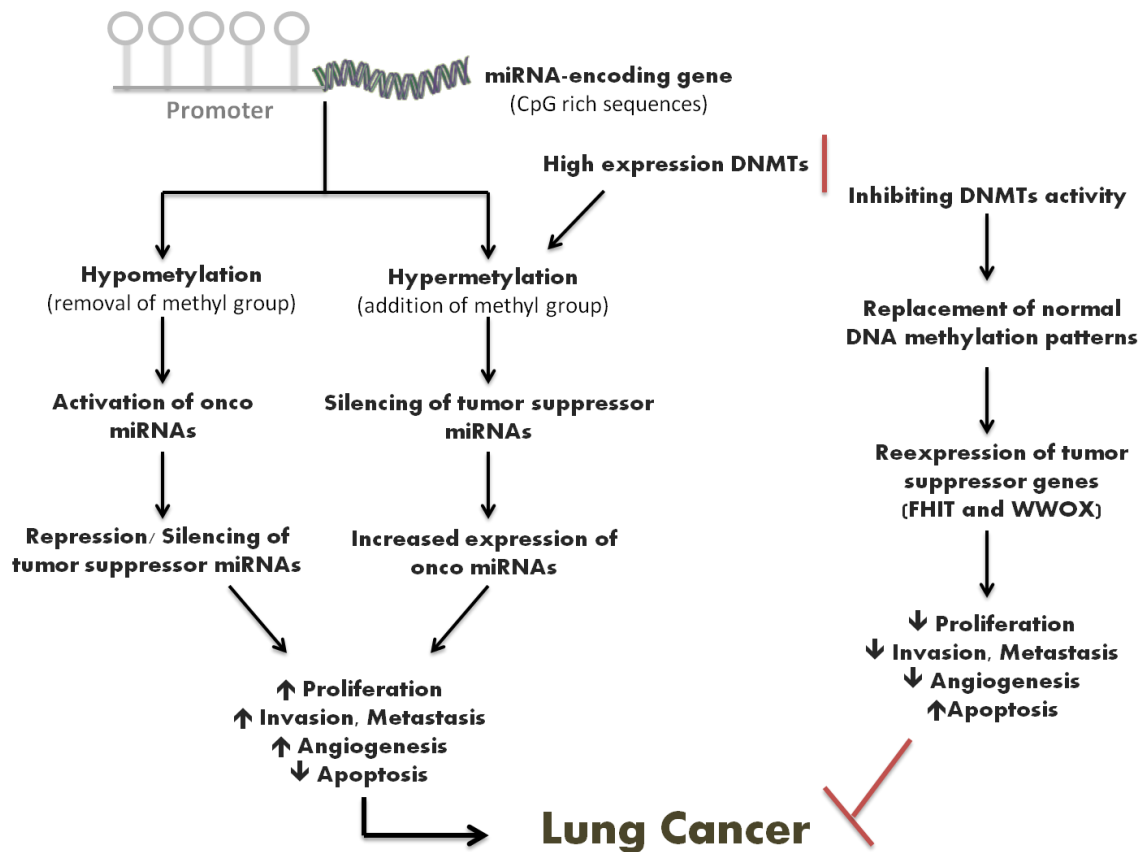


Figure 4. Regulation of miRNA expression by DNA methylation and its impact on lung tumorigenesis.

So, the purpose of this thesis is the development of a global strategy for the biosynthesis and purification of the recombinant human pre-miR-29b, to be delivered to non-small-cell lung cancer cells using suitable non-viral delivery systems, in order to normalize aberrant patterns of methylation (DNMT1 expression) in non-small-cell lung cancer cells involved in the insurgence and progression of the lung cancer.

CHAPTER II - Materials and Methods

2.1. Materials

For *E. coli DH5 α* culture, it was used tryptone and yeast extract from Bioakar (Beauvais, France), glycerol from Himedia, sodium chloride (NaCl) and dipotassium phosphate (K_2HPO_4) from Panreac (Barcelona, Spain), dipotassium phosphate (KH_2PO_4) from Sigma-Aldrich (St Louis, MO, USA), kanamycin from Thermo Fisher Scientific Inc. (Waltham, USA) and agar was from Pronalab (Mérida, Yucatán). GreenSafe Premium and Miniprep kit were purchased from NZYTech (Lisbon, Portugal). Guanidine thiocyanate salt, isoamyl alcohol and sodium citrate were from Sigma-Aldrich (St Louis, MO, USA), N-lauroylsarcosine from Fluka Analytical (United Kingdom) and isopropanol from Thermo Fisher Scientific Inc. (Waltham, USA). β -Mercaptoethanol, sodium acetate anhydrous and chloroform were from Merck (Whitehouse Station, USA) and glacial acetic acid was purchased from Chem-Lab (Zedelgem, Belgium). All chromatographic buffers were freshly prepared using 0.05% Diethylpyrocarbonate (DEPC, Acros Organics, New Jersey, USA) treated water and where filtered through a 0.20 μ m pore size membrane (Schleicher Schuell, Dassel, Germany). PEI ($M_w = 2$ kDa), CS medium molecular weight (MMW) ($M_w=190-310$ kDa, degree of deacetylation in the 75-85% range) were purchased from Sigma-Aldrich (St Louis, MO, USA). Stearic acid Grade I (98.5%), Lactoferrin human, 2-Iminothiolane hydrochloride (2-IOT, 98%), 1-ethyl-3-(3-dimethylaminopropyl) carbodiimide (EDC) and all cell culture media and reagents used in cell culture procedures were purchased from Sigma-Aldrich, unless otherwise noted.

2.2. Methods

2.2.1. Pre-miRNA-29 biosynthesis and isolation

The pre-miR-29b used in this study was obtained from a bacterial cell culture of *E. coli DH5 α* modified with the plasmid pBHSR1-RM containing the sequence of pre-miR-29b, as described by Pereira and collaborators [47]. Growth was carried out

in shake flasks (1000 mL) containing 250 mL of terrific broth culture medium (12 g/L tryptone, 24 g/L yeast extract, 0.017 M KH_2PO_4 , 0.072 M K_2HPO_4 and 4.7 mL/L glycerol), supplemented with 30 ug/mL kanamycin, at 37°C and 250 rpm. Cell growth was monitored by measuring the OD_{600} . Once the pre-fermentation growth reached an $\text{OD}_{600} \sim 2.6$ (exponential phase), a volume of culture was transferred into fermentation media. The volume transferred from pre-fermentation to fermentation was calculated in a way that the optical density of cells in the beginning of the fermentation would be of approximately 0.2 according to the equation (1).

$$V_{\text{from pre-fermentation}} = \frac{V_{\text{fermentation}} \times \text{OD}_{\text{fermentation}}}{\text{OD}_{\text{pre-fermentation}} - \text{OD}_{\text{fermentation}}} \quad (1)$$

OD was measured with Pharmacia Biotech Ultrospec 3,000 UV/Visible Spectrophotometer (Cambridge, England). Posteriorly, 50 mL aliquots of cell suspension were recovered by centrifugation at 3,900 *g* for 15 minutes at 4°C and stored at -20°C until use. RNA extraction was carried out based on the guanidinium thiocyanate-phenol-chloroform RNA isolation protocol [48]. The *E. coli DH5a* pellets (from 50 mL of culture medium) were thawed and resuspended with 0.8% sodium chloride solution. The suspensions were centrifuged at 6,000 *g*, 4°C for 10 minutes and the supernatant was discarded. Cell lysis was performed with 5 mL of solution D (4 M guanidine thiocyanate, 25 mM sodium citrate, 0.5% N-lauroylsarcosine and 0.1 M β -mercaptoethanol) and the lysates were resuspended by successive pipetting and incubated on ice for 10 minutes. Then, 0.5 mL of 2M sodium acetate pH 4 (prepared with sodium acetate anhydrous and glacial acetic acid) were added to the tubes, followed by a vigorous mixing and the sequential addition of 5 mL of water-saturated phenol, also followed by vigorous mixing and 1 mL of chloroform/isoamyl alcohol (49:1) mixed thoroughly, until two immiscible phases were obtained. Suspensions were incubated on ice for 15 minutes and centrifuged at 10,000 *g*, 4°C for 20 minutes. The supernatants were carefully pipetted into new lysis tubes and 5

mL of isopropanol was added to each tube for RNA precipitation, followed by a centrifugation (10,000 g, 4°C for 20 minutes). The supernatants were discarded and the pellets were resuspended with 1.5 mL of solution D by vortexing and precipitated with isopropanol (same volume of solution D). After the centrifugation at 10,000 g, 4°C for 10 minutes, the resulting pellet was washed with 75% ethanol (in DEPC water), incubated at room temperature for 15 minutes and centrifuged at 10,000 g, 4°C for 5 minutes. The pellets were dried at room temperature for 15-20 minutes and finally resuspended with 1mL of 0.05% DEPC-treated water. RNA concentrations were determined using a NanoPhotometer spectrophotometer (IMPLEN, United Kingdom). The samples were stored at -80°C.

2.2.2. Superporous-based arginine immobilization

For the arginine immobilization on the superporous matrix, it is first performed the swelling of the superporous support in water for two days. Then, 100 mg of matrix are added to 4 mL of sodium bicarbonate (NaHCO₃, 1M), pH 11, with 1 mL of Arginine 0.87 M, pH 9.5. The mixture should be allowed to stir for 72 hours, at 65°C. Completed the immobilization reaction the support is extensively washed with deionized water.

2.2.3. Pre-miRNA-29 purification

After small RNA extraction from *E. coli DH5α*, the recombinant pre-miR-29 samples were obtained by arginine affinity chromatography, using the previously prepared superporous-based arginine matrix column. The chromatographic experiments were performed in an AKTA Avant system with UNICORN™ 6.3 software (GE Healthcare, Sweden). The assays were performed at a flow rate of 1mL/min and the absorbance of the eluate was continuously monitored at 260 nm. The samples were injected into a 100 µL loop and eluted by using an increasing 1M NaCl in 10 mM Tris-HCl stepwise gradient in the different elution steps. The pooled fractions

were concentrated and desalted with Vivaspin 5,000 MWCO concentrators (Vivascience) and the samples were stored at -80°C for further analysis.

2.2.4. Agarose electrophoresis

The small RNA samples were prepared with loading buffer (bromophenol blue, glycerol and Tris Buffer) and injected in a 1% GSR agarose LE gel (Grisp, Porto, Portugal) stained with 0.01% GreenSafe Premium. Electrophoresis was carried out in 1x Tris-acetic acid (TAE) buffer (40 mM Tris-base, 20 mM acetic acid and 1 mM Ethylenediaminetetraacetic acid (EDTA), pH 8.0) and run at 120 V for 30 minutes. The gels were revealed under UV light in an UVITEC Cambridge Fire-reader XS D-56-26LM system (Cambridge, UK).

2.2.5. Polyacrylamide electrophoresis

The polyacrylamide gel electrophoresis was performed to analyze the integrity and to identify the RNA species present on the collected fractions. Samples were denatured with a formamide solution (97.5% formamide, 0.3% bromofenol, 10 mM EDTA at pH 7.5) at 55°C for 5 minutes and denatured conditions were kept in the gel due to the presence of 8 M urea. Electrophoresis was carried out at 140 V for 35 minutes with TBE buffer. The gel was stained with GreenSafe Premium 100 µL/L, (NZYTech, Lisbon, Portugal), for 15 minutes and was visualized using a UV transilluminator (UVItec, Cambridge).

2.2.6. Synthesis and characterization of PEI conjugated with Stearic Acid

The conjugation of PEI-SA and CS-SA were performed as previously reported by Xie and co-workers [97]. First, the SA (2.5 mg) and EDC (25 mg, at a ratio 1:10) were dissolved in 1.0 mL of anhydrous DMSO and stirred at 60°C for 1 hour, until EDC and SA were well-dissolved and mixed. The resulting mixture (SA:EDC) was then slowly added to 1% (w/v) of PEI 2 kDa and CS-MMW in sodium acetate buffer (0.1 M sodium acetate/0.1 M acetic acid, pH 4.5) and the reaction solution was kept at room

temperature in the dark during 24 hours, with stirring in a water bath. The amine group on PEI and CS was crosslinked with the carboxylic group of stearic acid by EDC as linker. Posteriorly, the resulting conjugate, PEI-SA/CS-SA, were dialyzed against double deionized water for 3 days, using dialysis membrane (SnakeSkin™ Dialysis Tubing MWCO 3500 Da, 22 mm dry diameter, ThermoScientific). The conjugated PEI-SA/CS-SA were isolated as a "sponge" by lyophilization and posteriorly, characterized by ¹H Nuclear Magnetic Resonance (NMR) spectroscopy.

2.2.7. Nuclear Magnetic Resonance (NMR) Spectroscopy

¹H NMR experiments were used to characterize and to confirm the chemical structure of PEI-SA / CS-SA complexes. All proton NMR spectra were performed at room temperature using a Bruker Avance III 600 operating at 600.10 MHz for protons, equipped with a QCI cryoprobe. All spectra were acquired under field-frequency locked conditions using that probe channel with the spectrometer's lock hardware. Spectra were processed using Bruker Topspin 3.2. All ¹H NMR spectra were referenced internally to the trimethylsilyl propionate signal in D₂O and tetramethylsilane in CDCl₃. Approximately, 10 mg of sample (CS-SA and PEI-SA) was placed in a 5-mm NMR tube (600 μL). Water suppression pulse using excitation sculpting with gradients (zgesgp) was used to reduce the ¹H signals of water.

2.2.8. Conjugation of sRNA with PEI-SA and CS-SA complexes

The polyplexes were formulated using the method of simple complexation between molar concentrations of positive charge, present in the protonated amine groups of polycation (N), and the negative charge of the phosphate groups of RNA (P) [109, 110]. To determine the specific N/P ratios, the mass of 325 Da corresponding to one phosphate group on small RNA was used. Moreover, over the pH used in this study, small RNA displays an approximately constant anionic charge density, with the pKa of the respective phosphate group close to 1.5 [111]. The calculation of the

positive charges was made in accordance with the pKa values and molecular weight of each polycation (Table 7).

Table 7. Main characteristics of polycations.

Polymer	Molecular weight (MW)	Monomer charge density	pKa [Ref]
PEI	2000	11 ⁺	9.26 [112]
CS-MMW	190000 – 310000	1 ⁺	6.5 [112]

Small RNA stock solution was prepared by RNA dissolution in sodium acetate buffer (0.1M sodium acetate / 0.1M acetic acid, pH 4.5), up to a final concentration of 20 µg/mL. The small RNA concentration was determined by NanoPhotometer spectrophotometer (IMPLEN, United Kingdom). The polycation stock solutions were also prepared in sodium acetate buffer pH 4.5 in a concentration of 10 mg/mL. Preliminary experiments were performed to identify the concentration range where the polyplexes are formed. A fixed volume of polycation solution (100 µL) of variable concentration was added to a small RNA solution (400 µL). The final concentration of small RNA was equal to 20 µg/mL and was kept constant in all the methods used for the characterization of the formed complexes. Particles were obtained by addition of cationic polymer solution to small RNA solution and immediately vortexed at soft speed for 1 minute. All the samples were subsequently left for equilibration at room temperature for 15 minutes. Finally, the polyplexes were recovery by centrifugation at 15,000 g, for 20 minutes, 4°C.

2.2.9. Particle size and zeta potential measurements

Measurements of average hydrodynamic particle size average (z-average), polydispersity index (PDI) and zeta potential of the polyplexes were performed in a Zetasizer Nano-ZS (Malvern Instruments, Worcestershire, UK). Before analysis, the

polyplexes were resuspended in deionized water and filtered. Size measurements were performed at 25°C with a backward scattering angle of 173°. The time-averaged autocorrelation functions were transformed into intensity-weighted distributions of the apparent hydrodynamic diameter using the available Malvern PCS software 6.20. The surface charges (zeta potential) of the polyplexes were performed in a zeta disposable folded capillary cells and determined by laser Doppler electrophoresis using a Zetasizer Nano ZS (Malvern Instruments Ltd., UK), at 25°C. The average values of size and zeta potential were calculated with the data obtained from three measurements \pm SD.

2.2.10. Scanning electron microscopy (SEM)

The morphological characteristics of the nanoparticles were visualized with a Scanning Electron Microscopy (SEM) (Hitachi S-3400N, Tokyo, Japan). Briefly, one drop of the solution containing the nanoparticles samples was placed on the surface of cover glasses and stored at 37°C overnight. Subsequently, the samples were then sputter coated with gold using an Bruker Nano, XFlash Detector 5010, Quorum-Q150R ES, for 3 min at 30 mA.

2.2.11. Determination of the encapsulation efficiency

The encapsulation efficiency (EE) of small RNA samples was calculated by determining free RNA concentration in the supernatant recovered after particle centrifugation (15,000 g, 20 minutes, 4°C) The amount of unbound small RNA was quantified by NanoPhotometer spectrophotometer (IMPLEN, United Kingdom). Supernatant recovered from unloaded complexes (without RNA) was used as a blank. Three repetitions of this procedure were performed for each system. EE% was determined using the following formula (2):

$$EE\% = \frac{\text{Total}(pre - sRNA \text{ amount}) - (pre - sRNA \text{ supernatant amount})}{\text{Total}(pre - sRNA)} \times 100 \quad (2)$$

2.2.12. Functionalization of PEI-SA and CS-SA with Lactoferrin

For the preparation of PEI-SA and CS-SA with Lf, Lf (10 mg) was dissolved in 1.0 mL aqueous solution of water and mixed with 0.5 mL aqueous solution of 2-iminothiolane hydrochloride (2-IOT, 0,7 mg) and the reaction proceed for 1 hour at room temperature with moderate shaking. Subsequently, PEI-SA and CS-SA were dissolved in 0.5 mL PBS (pH 7.0) and then added to the PBS solution of Lf, drop by drop, for 20 hours at room temperature, in the dark. To remove unreacted Lf, the resulting mixtures were purified by dialysis (SnakeSkin™ Dialysis Tubing, MWCO 3500 Da, 22 mm dry diameter, ThermoScientific) during 2 days against double deionized water and freeze dried, for further usage.

2.2.13. Sodium dodecyl sulfate-polyacrylamide gel electrophoresis (SDS- PAGE)

The SDS-PAGE was used to characterize the complexes PEI-SA-Lf and CS-SA-Lf, to confirm the functionalization with Lf. Reducing sodium dodecyl sulfate-polyacrylamide gel electrophoresis (SDS-PAGE) was performed, according to the method of Laemmli on a 10% polyacrylamide gel (Laemmli 1970). Samples were denatured by the addition of loading dye followed by incubation at 95°C for 10 minutes. Gel was stained by BlueSafe (NZYtech, Lisbon, Portugal). Low molecular weight protein marker (NZYtech, Lisbon, Portugal) was used as a molecular weight standard.

2.2.14. H1299 cell culture

The biological activity of pre-miR-29b was evaluated in an human non-small cell lung carcinoma cell line derived from the lymph node, H1299 (also known as NCI-H1299 or CRL-5803). These cells were cultured in the following medium: Dulbecco's Modified Eagle's Medium-High Glucose (DMEM-HG) supplemented with 10% (wt/vol) heat-inactivated fetal bovine serum (FBS) and 1% (wt/vol) penicillin-streptomycin. Cell lines were kept at 37°C in a humidified atmosphere containing 5% CO₂ and were detached by treatment with 1% trypsin-EDTA solution.

2.2.15. Transfection of H1299 cells with polyplexes (CS-SA-Lf/PEI-SA-Lf/pre-miR-29)

H1299 cells were seeded at a density of 5×10^4 cells per well in a 12-well plate. When a 50 to 60% confluence was achieved, the culture medium was replaced by serum-free medium. After 12 hours, polyplexes were added to the cells at pre-miR-29 concentration of 10 nM and transfection was carried out during 4 hours. The culture medium was replaced by fresh medium supplemented with 1% antibiotic, to allow the cells to remain metabolically active, expressing DNMT1. Untreated cells were used for negative controls. The cells were harvested 48 hours after transfection. All transfection experiments were performed in triplicate.

2.2.16 Expression of DNMT1 mRNA in H1299 cells by RT-qPCR

Total RNA was extracted from the cells using TRIzol reagent (Invitrogen). 1 μ g of total RNA was reverse transcribed using the RevertAid First Strand cDNA Synthesis Kit (Thermo Fisher Scientific Inc.), according to the manufacturer's instructions. For quantitative analysis, RT-qPCR amplification of cDNA was performed using the Maxima® SYBR Green/Fluorescein qPCR Master Mix (Thermo Fisher Scientific Inc.) in an IQ5 Cyclor from BioRad. RT-qPCR efficiencies were calculated from the given slopes with MyIQ 2.0 software (BioRad). The relative quantification of the DNMT1 expression was based on the comparative threshold cycle (C_T) method in which the amount of the target was determined to be $2^{-(\Delta C_T \text{ target} - \Delta C_T \text{ calibrator})}$, normalized to levels of glyceraldehyde-3-phosphate dehydrogenase (GAPDH) and relative to the untreated control cells. The primers used in these experiments were 5'- CGA CTA CAT CAA AGG CAG CAA CTT G -3' (forward) and 5'- TGG AGT GGA CTT GTG GGT GTT CTC-3' (reverse) for the amplification of human DNMT 1 and 5'- CCTGGGTGTAGGGCACATAC - 3' (forward), 5'-AGTGTAGCCCAAGATGCCCTTCAG- 3' (reverse) for the amplification of GAPDH. Each sample was run in triplicate, and threshold cycle (C_T) values were averaged from the triplicate. The final data were averaged from 3 separately conducted experiments.

CHAPTER III - Results and Discussion

3.1. Recombinant pre-miR-29 production and isolation

In this work, the *E. coli DH5α* cells transformed with pBHSR1-RM-pre-miR-29 plasmid were cultivated, allowing the replication of the plasmid, and consequently the expression of the precursor of recombinant miRNA (pre-miR-29), according to the process depicted in Figure 5. In comparison with the chemical synthesis of RNAs, this strategy, used to biosynthesize pre-miRNAs using the bacterium *E. coli*, resulted in an improvement of RNA production and quality with a less time-consuming and less expensive procedure, once this host can be grown easily and economically [113].

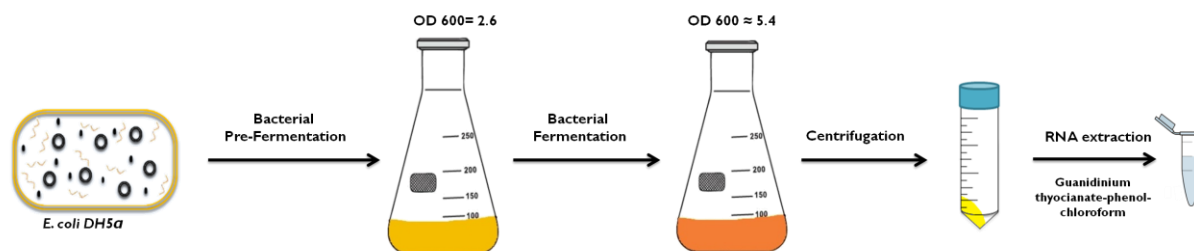


Figure 5. Global process employed in this work for the recombinant biosynthesis and isolation of RNAs from *E. coli DH5α*.

The time course profile, in Figure 6, represents the bacterial growth during the fermentation process. It is possible to observe that the experimental conditions applied promoted the growth of the bacterium until reaching optical densities of 5.392 ± 0.109 after 6 hours of cultivation. After this cultivation time, it was observed a slight decrease of the bacterial growth, outcome of the consume of nutrients during the exponential phase. In this final phase, the lack of nutrients in the culture medium leads to metabolic stress and, afterwards, to the cell death.

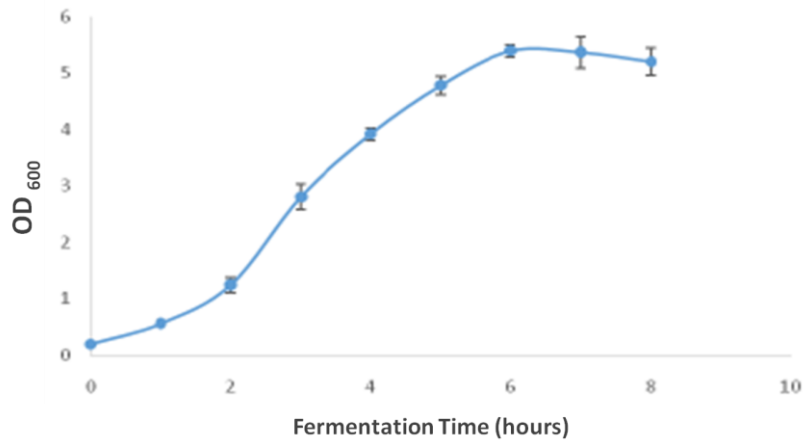


Figure 6. Representative growth curve of *E. coli* DH5a holding the pBHSR1-RM-pre-miR-29. Each value represents the mean of three independent samples.

After the fermentation, the cells were recovered by centrifugation and the *E. coli* DH5a sRNA fraction containing the pre-miR-29 was extracted by the acid guanidinium thiocyanate-phenol-chloroform method [48]. Posteriorly, an agarose gel electrophoresis was carried out to verify the RNA integrity and to confirm if these samples were contaminated with genomic DNA (gDNA), as it is shown in Figure 7A. In addition, these samples were also analyzed by polyacrylamide electrophoresis, as shown in Figure 7B. Typically, the profile of sRNA comprise the pre-miR-29 (110 bp), but also the 6S RNA (184 bp), and tRNA species (typically between 73 to 94 bp).

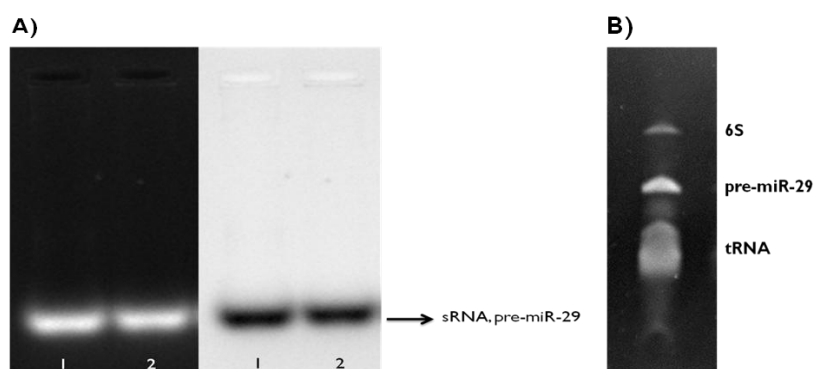


Figure 7. A) Agarose gel electrophoresis of total RNA extraction containing recombinant pre-miR-29 from *E. coli* DH5a. The lanes 1 and 2 correspond to RNA samples obtained from two independent RNA extractions. **B)** Polyacrylamide electrophoresis of sRNA sample, with the mixture of RNA species (6S, pre-miR-29 and tRNA).

In this way, considering the complexity of the sample, due to the presence of different RNA species, it is necessary the use of purification methods to isolate the biomolecule of interest, in this case, the pre-miR-29. The purification methods are a critical step to obtain the product with suitable quality to be applied in several biomedical fields.

3.2. Superporous matrix functionalization with arginine

The purification methods developed to purify microRNAs require the use of a chromatographic support to eliminate impurities, but simultaneously able to maintain the structural integrity of this biomolecule. Some affinity chromatographic strategies have been extensively employed for RNAs purification in our research group. Indeed, distinct amino acids, such as lysine, tyrosine and arginine amino acids have been successfully applied as affinity ligands for pre-miR-29 purification, in conventional particle-based columns [60–62].

In affinity chromatography, different affinity ligands (amino acids and its derivatives, peptides, complementary oligonucleotides sequences to the target miRNAs, among others), can be characterized and immobilized onto different chromatographic matrices (agarose-based, monoliths, superporous matrices), envisaging the purification of the biomolecule of interest from the remaining host contaminants. With the purification of the target RNA it is also expected to minimize non-targeted gene silencing effects and immunologic responses upon application.

Accordingly, the present study was developed to explore not only the natural interactions that occur between the arginine and the pre-miRNA, as previously mentioned, but also to explore the advantages of using a superporous matrix (Figure 8), thereby conjugating the selectivity, specificity and biorecognition of arginine ligands with the structural versatility and capacity provided by superporous matrix.

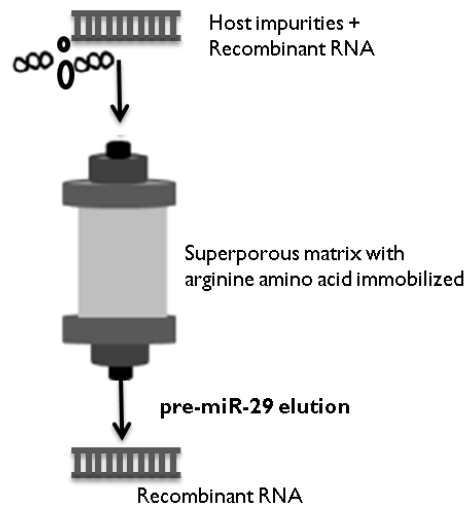


Figure 8. Affinity purification strategy for recombinant RNA isolation with a superporous-arginine column.

Thus, the superporous matrix was properly modified with arginine ligand, immobilized by the epoxy group. The suitable arginine immobilization was confirmed through a comparison of the chromatographic profiles obtained by loading a RNA sample on the superporous matrix support and the superporous matrix support with arginine immobilized.

These two matrices were equilibrated with 10 mM Tris-HCl buffer (pH 8.0), previous to the injection of a sRNA sample (40 $\mu\text{g}/\text{mL}$). The Tris-HCl condition was maintained to elute unbound species, and then the mobile phase was changed to 1 M of NaCl in 10 mM Tris-HCl buffer (pH 8.0) to recover the biomolecules retained on the columns. Several fractions were recovered along the chromatographic runs and the absorbance at 260 nm was monitored to conclude about the sRNA binding/elution profiles. In figure 9, the chromatogram A represents the result achieved with the superporous matrix, in which a single peak was attained in the flow through due to the immediate elution of RNA species. This result indicates that the sRNA molecules did not interact with superporous matrix under the conditions used.

In the chromatographic profile represented in figure 9B, it was verified that the matrix modified with the arginine ligand, promoted the total retention of sRNA at 10 mM in Tris-HCl buffer (pH 8.0). Posteriorly, the total elution was verified when the

NaCl concentration was increased to 1 M. These results prove the successful immobilization of arginine, indicating that the superporous matrix with arginine is chemically different from the superporous matrix and the interaction and retention of the sRNA onto the support is due to the arginine ligands.

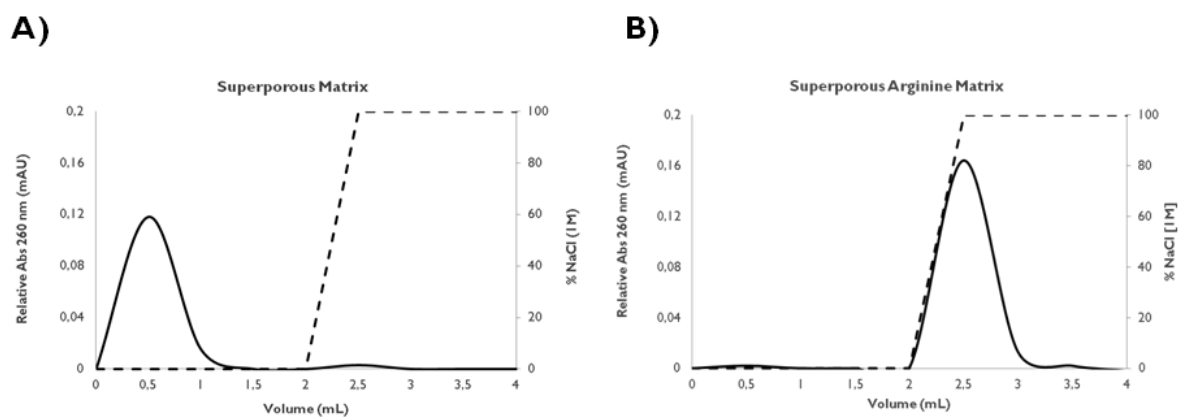


Figure 9. Chromatographic profiles of sRNA interaction with superporous matrices. **A)** Superporous matrix without arginine immobilized; **B)** Superporous matrix modified with the arginine ligands.

The elution was performed by increasing the NaCl concentration from 0 M to 1 M. The dashed line indicates the gradient of the NaCl concentration.

3.2.1. Purification of pre-miR-29 with the superporous-arginine matrix

Based on the previous knowledge about the purification of pre-miR-29 in arginine-based matrices, in this work it was evaluated the application of the superporous-arginine support. So, aiming to favor mainly ionic interactions, after binding in low salt concentration conditions, the pre-miR-29 elution was achieved with the application of an increasing stepwise gradient of NaCl in 10 mM Tris-HCl buffer, as it was previously described by Pereira and co-workers for the isolation of pre-miR-29 by arginine affinity chromatography [60].

The initial experiments were performed to determine the best binding/elution strategy for pre-miR-29 using a gradient of NaCl. The chromatographic profile of the pre-miR-29 purification from a complex mixture of *E.coli* sRNAs is presented in figure 10, and the presence of different peaks in the chromatogram indicates that the RNAs

present in the sRNA population interacted differently with the superporous-arginine support. The chromatographic assay was initiated with 110 mM NaCl in 10 mM Tris-HCl buffer (pH 8.0). After injection of the complex mixture of sRNA (20 μ g/mL), a first peak was obtained with the same salt concentration of the equilibrium buffer (figure 10A, peak 1), resulting from the elution of unbound species (figure 10B, lane1). The ionic strength of the elution buffer was then increased to 300 mM of NaCl to elute the pre-miR-29 in the second step. Moreover, the elution of highly bound species was achieved by increasing the ionic strength of the buffer to 1 M NaCl in 10 mM Tris-HCl (figure 10A, peak 3). The peak 3 obtained with 1M NaCl, with approximately 30 mAU, refers mainly to low molecular weight RNA species (tRNAs), as revealed by the electrophoretic analysis (figure 10B, lane 3).

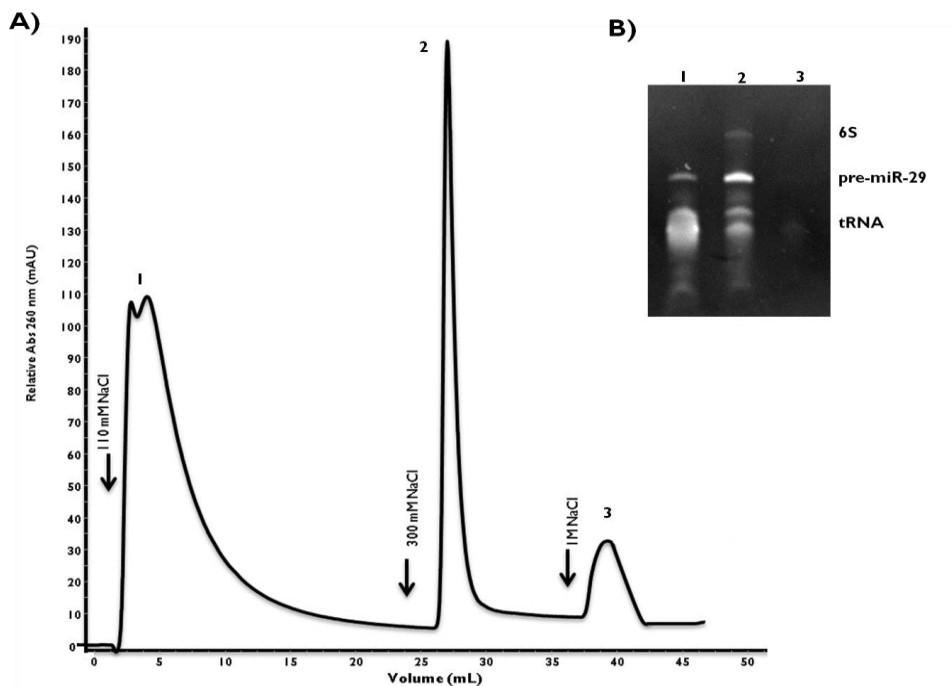


Figure 10. A) Chromatographic profile of the pre-miR-29 purification from a sRNA mixture using the superporous arginine matrix.

Elution was performed at 1.0 mL/min by using a stepwise NaCl gradient in 10 mM Tris-HCl buffer in the eluent, increasing the salt concentration from 110 mM, to 300 mM and 1 M, as represented by the arrows. **B)** Polyacrylamide gel electrophoresis of samples eluted from the column. Fractions corresponding to peaks 1–3 are shown in lanes 1–3, respectively.

In an attempt to improve the pre-miR-29 recovery yield in the second chromatographic step, the NaCl concentration in the binding step was lowered. So, the first peak of this chromatographic run, was obtained with 105 mM of NaCl in 10 mM Tris-HCl (figure 11A, peak 1). Then, the elution of the bound species was performed with 150 mM NaCl (figure 11A, peak 2) and in a third step, by applying 500 mM NaCl (figure 11A, peak 3), some contaminants were eluted. Through the analysis and comparison of the binding steps of these two chromatographic experiments, it was observed that with 105 mM NaCl, less pre-miR-29 quantity was eluted in this initial step, thereby increasing the recovery yield in the second gradient step, with 150 mM NaCl (figure 11B, lane 2). Also, analyzing both electrophoresis, it was verified that, in the peak 3 some more low molecular weight contaminants were eluted, in comparison with the previous experiment, which can contribute for the relative purity of pre-miR-29 fraction.

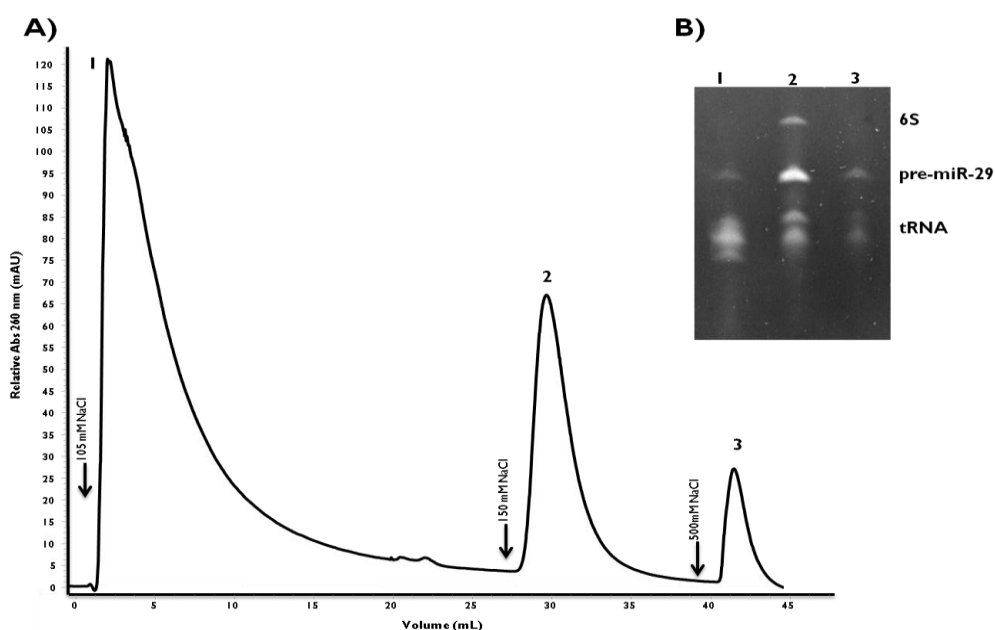


Figure 11. A) Chromatographic profile of the pre-miR-29 purification from a sRNA mixture using the superporous arginine matrix.

Elution was performed at 1.0 mL/min by using a stepwise NaCl gradient in 10 mM Tris-HCl buffer in the eluent, increasing the salt concentration from 105 mM, to 150 mM and 500 mM, as represented by the arrows. **B)** Polyacrylamide gel electrophoresis of samples collected at the column outlet. Fractions corresponding to peaks 1–3 are shown in lanes 1–3, respectively.

In the chromatographic assay represented in Figure 12, the superporous-arginine column was equilibrated with 100 mM NaCl in 10 mM Tris-HCl buffer, trying to promote the elution of small weight RNA species (tRNAs) and 6S RNA and the retention of pre-miR-29. After the binding step, the elution of the target RNA was performed by increasing the ionic strength to 130 mM NaCl, to recover higher quantity of pre-miR-29 and to avoid the elution of many low molecular weight contaminants. To obtain the third peak, the NaCl concentration was increased to 500 mM of NaCl, for the elution of some additional RNA contaminants. In figure 12B, the electrophoretic profile presented in lanes 1, 2 and 3 corresponds to the samples pooled from the respective peaks in the chromatogram. Hence, the electrophoretic analysis showed that the first peak of unbound species mainly corresponds to the elution of transfer RNA (tRNA) species (figure 12B, lane 1), while the second peak mainly refers to the pre-miR-29 (figure 12B, lane 2), reaching some purity degree. Finally, the third peak refers to tRNA species and some pre-miR-29 which was retained in the column (figure 12B, lane 3).

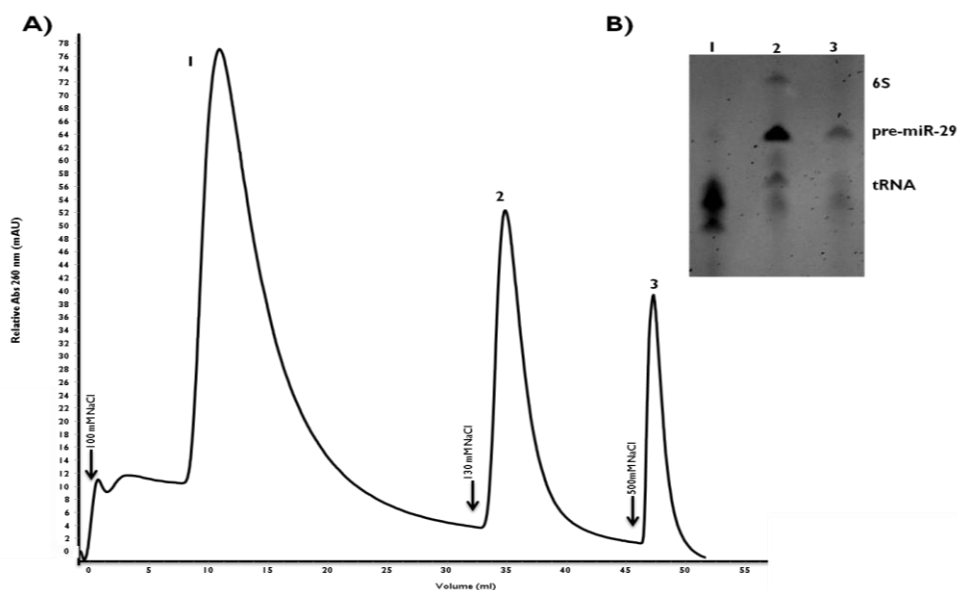


Figure 12. A) Chromatographic profile of the pre-miR-29 purification from a sRNA mixture using the superporous arginine matrix.

Elution was performed at 1.0 mL/min by using a stepwise NaCl gradient in 10 mM Tris-HCl buffer, increasing the salt concentration from 100 mM, to 130 mM and 500 mM, as represented by the arrows. **B)** Polyacrylamide gel electrophoresis of samples collected at the column outlet. Fractions corresponding to peaks 1–3 are shown in lanes 1–3, respectively.

These results suggest that the pre-miR-29 presents a wide ability to bind the superporous-arginine matrix, establishing a strong interaction with this support. The electrostatic interactions could play an important role on RNA retention, but the interactions between the nucleotides bases and the arginine ligand are also involved and modulate some favored interaction and specificity.

The pre-miR-29 structural features explain the specific interactions occurring between the pre-miR-29 and the immobilized arginine. The single-stranded nature of RNA is normally involved in RNA recognition, due to the higher bases exposure and availability for interactions. Pre-miR-29 is a sRNA molecule in the shape of a stem-loop or hairpin consisting of two long irregular double-stranded stem regions, which are interrupted by a largely single-stranded internal loop. The continuous stem sequences which exists along the bulge, present several guanines, which are able to interact preferentially with arginine [53].

On the other hand, arginine offers the possibility to promote a multiposition interaction with RNA sites and this phenomenon occurs because this amino acid has two different polar centers with which RNA can strongly associate: at α -carbon group and the guanidinium side chain [114, 115]. Thus, it is reasonable to explain that the retention of RNA in the superporous-arginine matrix is due to arginine side chain, which can promote multicontacts with RNA backbone or RNA bases, according to RNA folding.

In general, the elution strategy with NaCl showed to be propitious for pre-miR-29 purification in this support, comparatively to other strategies already tested by the group, namely in comparison with the method described by Pereira and co-workers, involving the purification of pre-miR-29 with agmatine affinity chromatography, where higher salt conditions were used to elute bound species [67].

Based on this, it can be concluded that the arginine amino acid presented promissory results in comparison with the agmatine, namely regarding the salt concentration needed in the mobile phase, which is considerably lower than those typically used in other chromatographic techniques, to obtain the target RNA. The application of arginine can also be advantageous, as it is strongly associated with the

preserved integrity observed in RNA. Actually, owing to the multiplicity for interactions that can be promoted, arginine has been largely associated with stabilizing effects on RNA conformation [67].

However, considering the presented results, it is also important to refer that the strategy used in this study for pre-miR-29 purification can be improved in the future, in order to achieve a higher purity degree for the target RNA. The affinity chromatography can be considered a very good approach to purify these nucleic acid molecules due to the wide advantages it presents in comparison to other RNA purification chromatographic strategies, such as, the hydrophobic or electrostatic chromatography and affinity tags [13, 55, 61, 62, 117].

After the purification of pre-miR-29, the delivery of this therapeutic biomolecule remains a considerable hurdle due to the rapid enzymatic digestion in plasma and renal elimination, limited penetration across the capillary endothelium and inefficient uptake by tissue cells. So, it is critical to be able to control the level of the drug and the duration of its action, such that the exposure is safe while still being efficacious. To overcome these drawbacks, some delivery systems were developed, called polyplexes, to encapsulate and carry the therapeutic molecule to the target cells.

3.3. Synthesis and characterization of PEI-SA, CS-SA, CS-SA-Lf and PEI-SA-Lf complexes

In general, the association of RNA with the polymeric systems increases the protection of the target biomolecule, however other features can also be controlled and optimized in order to improve the general characteristics of these systems. Thus, the polyplexes formed by PEI and CS, were initially functionalized with SA, aiming an increase of their circulation time, when in contact with the body fluids. The carriers of PEI-SA/CS-SA were synthesized by chemical reaction between the carboxil group of SA and the amino groups of PEI/CS in the presence of EDC, a carboxil activating agent [97].

Posteriorly, these polyplexes were analyzed by several techniques, in order to characterize their chemical and structure properties.

3.3.1) ^1H NMR analysis

In order to confirm the modification of PEI and CS with SA and to characterize the chemical structure of PEI-SA/CS-SA complexes, ^1H NMR experiments were performed.

The PEI and CS spectra were also recorded without SA, for comparison purposes. The ^1H NMR spectrum of the PEI was assigned and the proton peaks of PEI ($-\text{NHCH}_2\text{CH}_2-$) appeared at 3.2–2.0 ppm. The analysis experiments indicate that the amino-groups of the PEI were acylated (figure 13).

Then, the molecular structure of PEI-SA was confirmed by ^1H NMR spectroscopy. The ^1H -NMR assignment of PEI-SA was as follows: δ (ppm): 0.86–0.89 (t, $-\text{CH}_2\text{CH}_2(\text{CH}_2)_{15}\text{CH}_3$), 1.25 (br, $-\text{CH}_2\text{CH}_2(\text{CH}_2)_{15}\text{CH}_3$), 1.62 (br, $-\text{CH}_2\text{CH}_2(\text{CH}_2)_9\text{CH}_3$), 2.18 (br, $-\text{CH}_2\text{CH}_2(\text{CH}_2)_9\text{CH}_3$), 2.39–3.3 (m, $-\text{CH}_2\text{CH}_2\text{NH}-$, $-\text{CH}_2\text{CH}_2\text{N}-$, $-\text{CH}_2\text{CH}_2\text{NHCO}-$, $-\text{CH}_2\text{CH}_2\text{NHCO}-$). The ratio between the peak area at 3.0–2.4 ppm and the peak area of the methyl group in PEI-SA was bigger than that of PEI (figure 14). These results indicated that SA was successfully linked to PEI.

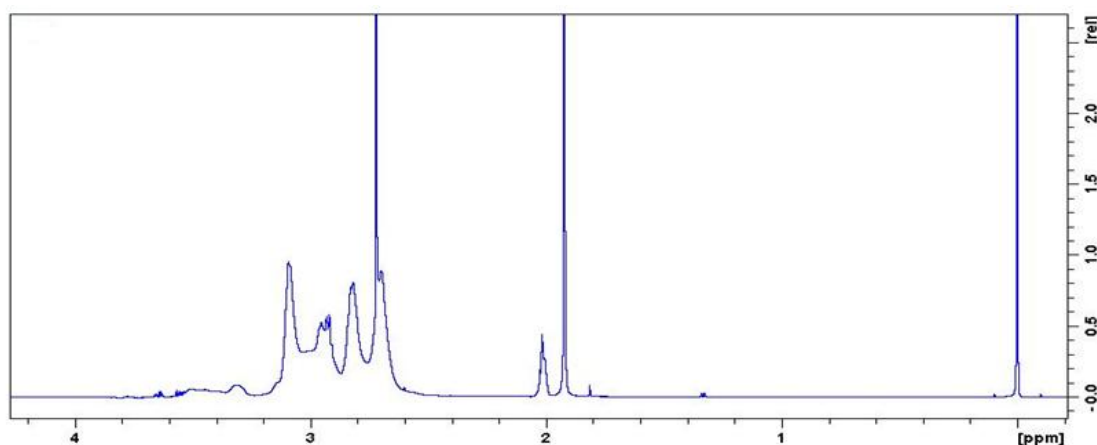


Figure 13. PEI ^1H NMR spectrum without SA.

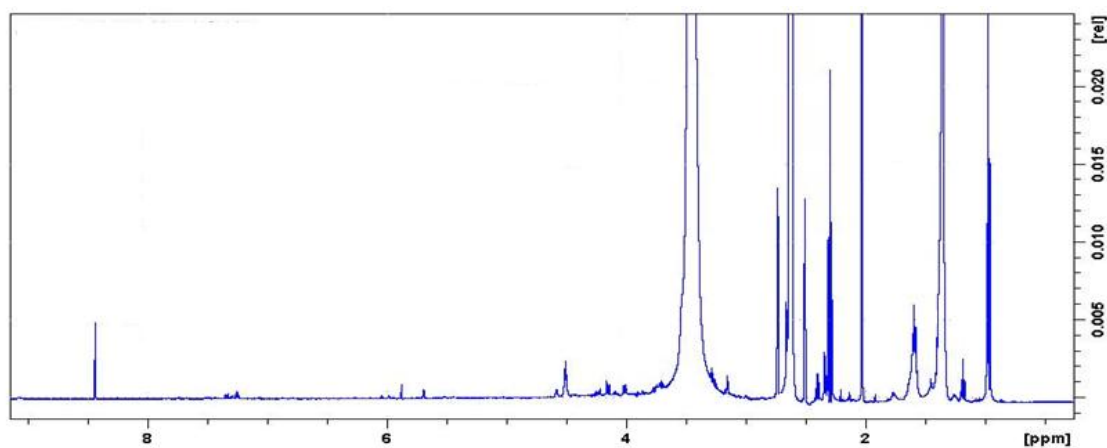


Figure 14. SA and the amino group of PEI in the presence of EDC, a carboxyl activating agent.

The ^1H -NMR assignment of CS was previously determined and was as follows:
 ^1H NMR (CS, D_2O) = 5.10 (H_1), δ = 3.09 (H_2), δ = 3.43 \approx 3.81 (H_3 , H_4 , H_5 , H_6), δ = 1.96 (NHCOCH_3) ppm (figure 15).

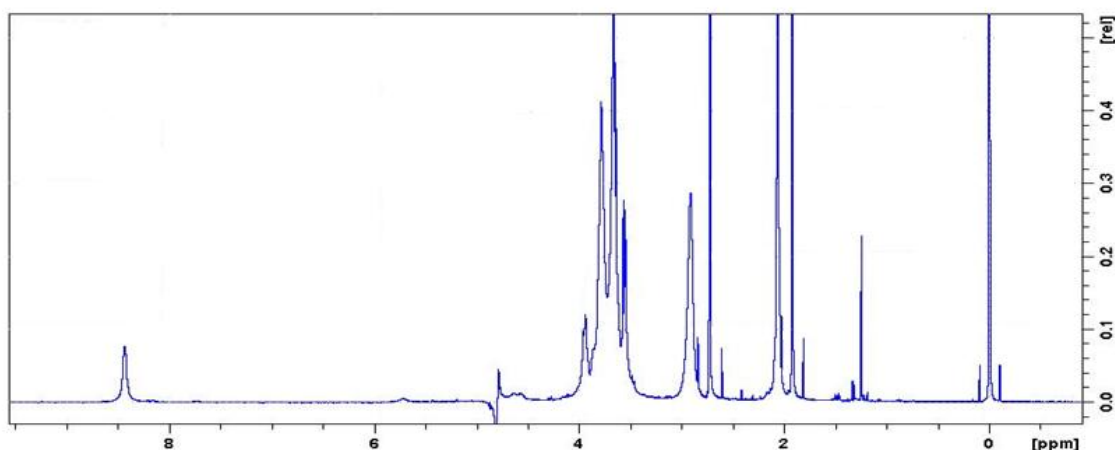


Figure 15. CS ^1H NMR spectrum without SA.

Comparing CS with CS-SA ^1H -NMR spectra, it was verified that the presence of the triplet signals at 0.9 ppm, due to the terminal CH_3 protons of SA, and the new signal between 1–1.5 ppm corresponding to the CH_2 chain of the acyl chain, corroborates that SA was linked to CS (figure 16).

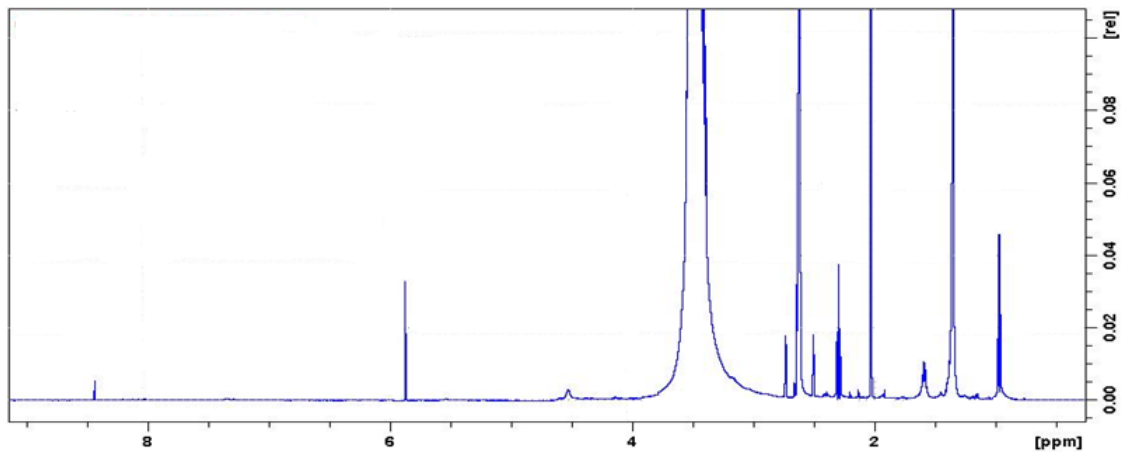


Figure 16. SA and the amino group of CS in the presence of EDC, a carboxyl activating agent.

3.3.2) Structural properties of PEI-SA and CS-SA complexes

Through the structures of different polycations, it is possible to determine the average size and charge density of the respective monomers. Considering the molecular weight of each monomer and the corresponding average chain molecular weight, it is possible to estimate the number of monomers per chain, $N_{\text{mon,PC}}$. As demonstrated in the table 7, in *Material and Methods* chapter, the highest charge density is expected for PEI polymer, once it shows the high monomer charge density, with eleven positive charges. The CS chains display the highest chain length, due to the molecular weight between 190000-310000 Da, but the lowest charge density, with an unique positive charge. The pKa values that the polycations possess are higher than those of the RNA phosphate groups, close to 1.5 [111].

In the complexes preparation, the polycations were mixed with sRNA at several ratios for the formation of sRNA-polycations particles (polyplexes) in acetate buffer at pH 4.5. This pH was chosen because it fits within the range of pH values that has been attributed to the endo/lysosomal compartments. Additionally, at this value, the amine groups of polycations used in this study are protonated and act as a cationic polyelectrolyte, which can interact with the negatively charge of pre-miR-29.

According to the electrophoretic analysis shown in Figure 17, it was observed that the lanes corresponding to the N/P ratios of 2.5, 5 and 7.5 contain free sRNA in

the PEI/sRNA complex. However, above the N/P ratio of 7.5, the bands corresponding to free sRNA were not observed, indicating that the sRNA was conjugated with the PEI polymer (figure 17).

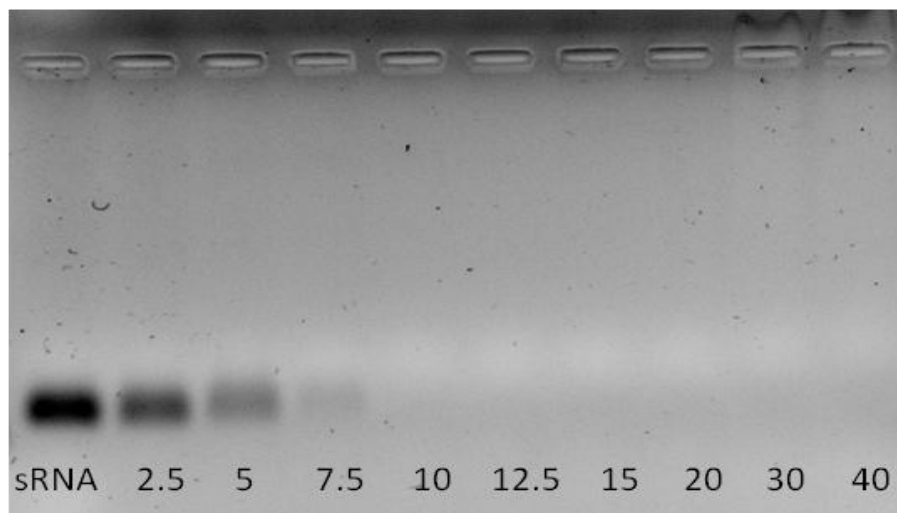


Figure 17. Agarose gel electrophoresis of sRNA/PEI polyplexes at various N/P ratios. The first lane of the gel corresponds to free sRNA. The numbers in each lane indicate the N/P ratios values. Each experiment was performed three times.

According to Figure 18, the encapsulation studies of PEI/sRNA are in agreement with the agarose electrophoresis above, once in the three initial ratios - N/P=2.5, N/P=5 and N/P= 7.5 -, the lowest values of encapsulation were observed, while at the N/P ratios 10-40, about 100% of sRNA loading efficiency was achieved. At this point, sRNA is completely complexed with PEI (2kDa) (figure 18). Through the analysis, it was also confirmed that more than 90% of sRNA loading efficiency was achieved with the N/P ratio 10 (figure 18). It is known that polycations with higher charge densities promote the strongest binding with RNA [118]. The branched structure of this PEI can promote a more efficient interaction with sRNA. Indeed, some studies have also pointed that, when a linear polymer structure is compared with a branched structure, the branched structure may be beneficial for the interaction with sRNA [119].

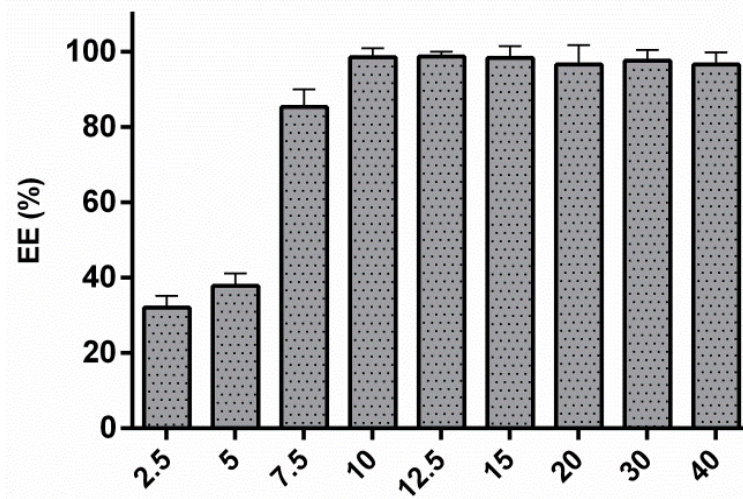


Figure 18. Encapsulation efficiency of sRNA/PEI polyplexes at various N/P ratios. The mean results and standard deviations of three independent measurements are presented (mean \pm SD are given, three repetitions each).

In the case of CS-MMW, was demonstrated that the sRNA complexation starts at very low values of N/P ratio. This condensation becomes at N/P ratio 2.5 until 50, suggesting that sRNA is fully complexed, as seen in the electrophoresis – figure 19.

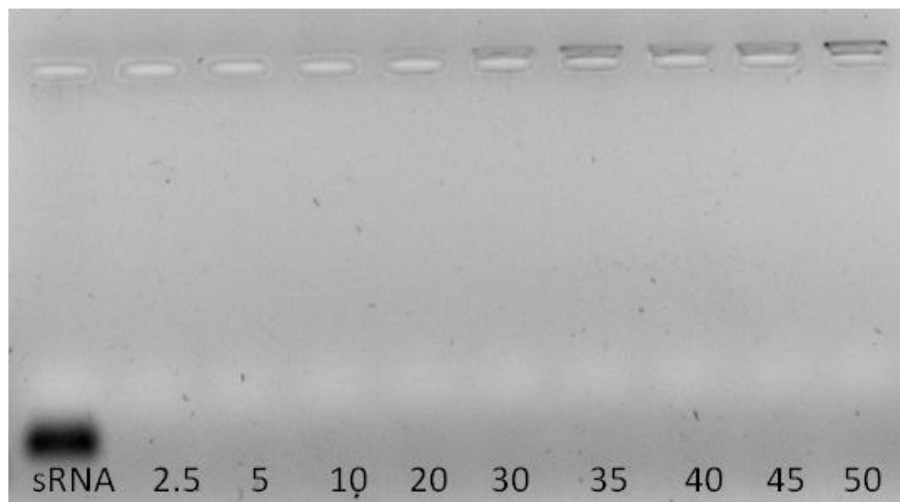


Figure 19. Agarose gel electrophoresis of sRNA/CS polyplexes at various N/P ratios. The first lane of the gel corresponds to free sRNA. The numbers in each lane indicate the N/P ratios values. Each experiment was performed three times.

These results also corroborate with the encapsulation efficiency study, once in every N/P ratios of sRNA/CS, high encapsulation efficiency values were achieved, being higher than 80% for all the cases (figure 20). These observations suggest that CS can be more efficient in sRNA condensation than PEI, which can be probably due to the different interaction of RNA with CS or PEI. Although the CS possesses a low charge density, the sRNA is neutralized and completely surrounded by the positive charges, due to its long chains [112].

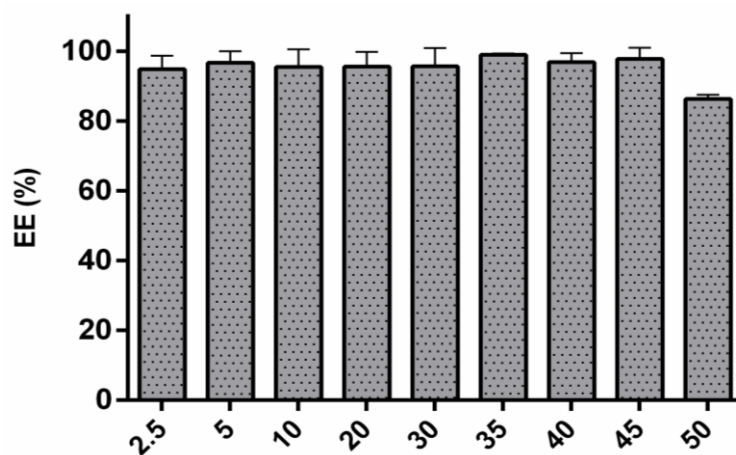


Figure 20. Encapsulation efficiency of the sRNA/CS polyplexes obtained from various N/P ratios.

The mean results and standard deviations of three independent measurements are presented (mean \pm SD are given, three repetitions each).

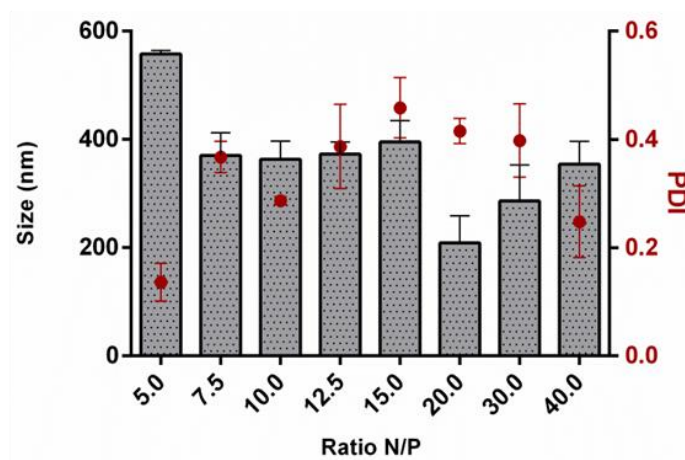
In what concerns to complexes preparation, the particle size and surface charge are two important factors with an enormous influence on the particle stability and cell adhesion. The characterization of the relevant parameters such as size and zeta potential were determined at various N/P ratios of sRNA with polycations PEI (2kDa) and CS-MMW.

Figures 21 shows the sizes for different N/P ratios of PEI conjugated with sRNA, determined by dynamic light scattering (DLS). The values of size and zeta potential were calculated with the data obtained from three independent measurements (mean \pm n=3). In the absence of polycation, the sRNA presents a size of about 325 nm. On the other hand, when the sRNA was complexed with PEI, for the

lowest ratios, it demonstrated higher size, contrasting with higher polymer values (figure 21A). This may be due to the fact that at the lowest ratios, the sRNA is not fully conjugated, which may contribute to increased particle size.

In figure 21B, it is exemplified one particular sample, where it is shown that sRNA/PEI presents a size between 200 nm to a 400 nm. The particles should have an approximately size with 260 nm, to cross the endothelial cells of the lung capillary bed and do not suffer uptake by the macrophages [120].

A)



B)

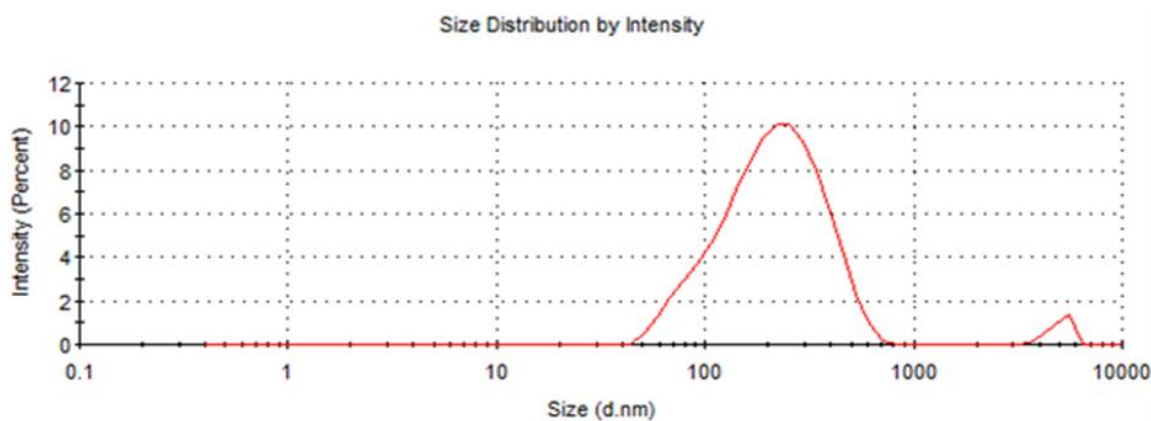


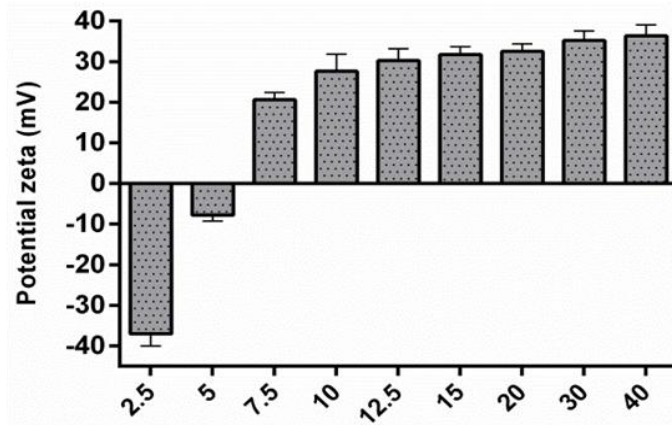
Figure 21. A) Particle size for different N/P ratios of PEI (2kDa) conjugated with sRNA.

B) Measurement size distribution of one sample, to confirm the small particles, between 200-400 nm.

The values of size were calculated with the data obtained from three independent measurements (mean \pm SD, n = 3).

Concerning the zeta potential, it was observed a gradual increase in the charge of the complexes - from negative to positive values -, as the amount of polymer increases. The complexes formed with sRNA at the lower N/P ratios (2.5, and 5) displayed negative zeta potentials (figure 22A), indicating that the RNA is not fully complexed with the polycation, and they are in accordance with the results obtained in the electrophoresis (figure 19). These results may be due to the fact that most of the positively charged PEI chains in PEI/sRNA complexes were closely covered with the strongly anionic RNA. Thus, according with these results, the N/P ratios that could be chosen for a possible application, should be above the 7.5 ratio, once these systems showed a high positive charge, which will facilitate cell transfection. The cell membrane presents negative charge and the contact with positively charged polyplexes is mediated by electrostatic interactions, enabling the particles entrance into the cell and preventing the particle aggregation.

A)



B)

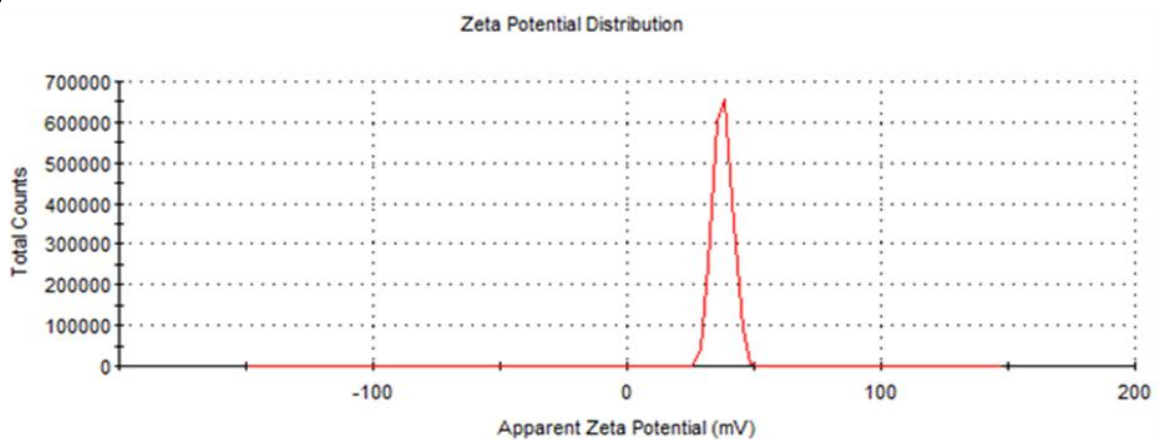
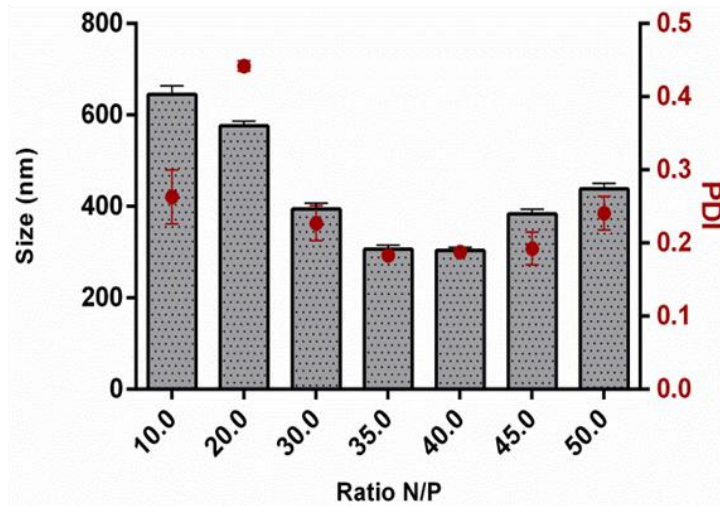


Figure 22. A) Zeta potential analysis for different N/P ratios of PEI (2kDa) conjugated with sRNA. **B)** Measurement of zeta potential distribution to confirm the defined charge of the particle.

The values of zeta potential were calculated with the data obtained from three independent measurements (mean \pm SD, n = 3).

Regarding the CS-MMW, in general, the size values are slightly higher than those obtained with PEI. In particular, the ratios 10 and 20 showed the highest size values, about 600 nm, while the ratios with the lowest size, were the 35 and 40 ratios, approximately 300 nm (figure 23A). The sizes of CS-based systems, to the different ratios, are larger than for the PEI polymer, can be explained by the fact that CS is also a large polymer [121].

A)



B)

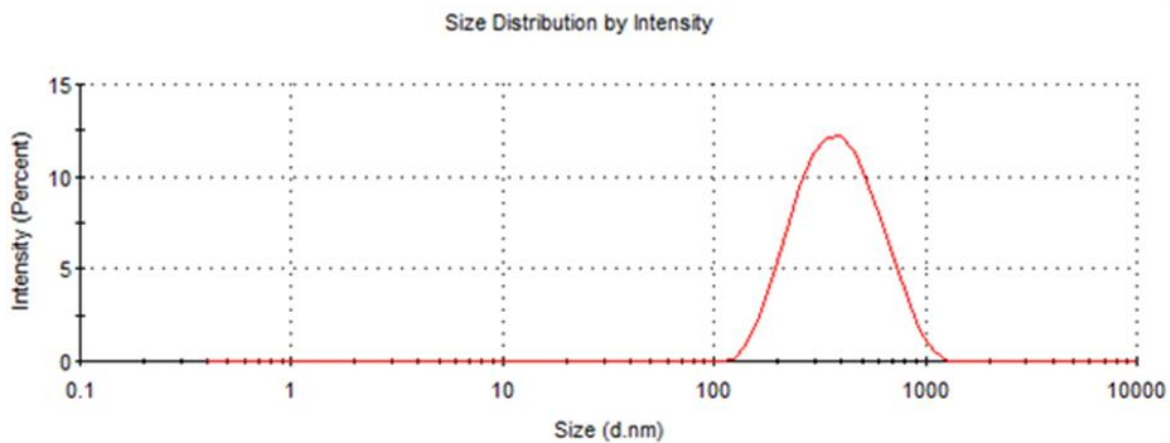


Figure 23. A) Particle size for different N/P ratios of CS-MMW conjugated with sRNA.

B) Measurement size distribution of one sample, to confirm the small particles, between 300-400 nm.

The values of size were calculated with the data obtained from three independent measurements (mean \pm SD, n = 3).

The study of zeta potential of sRNA/CS systems revealed that they present positive charge in all studied ratios. The zeta potential values are also higher, comparatively to the values obtained with PEI polymer. In figure 24, it is also observed a slight increase of zeta potential value as the ratio increases, and, above the ratio of 20, the values are almost constant and near 40 mV.

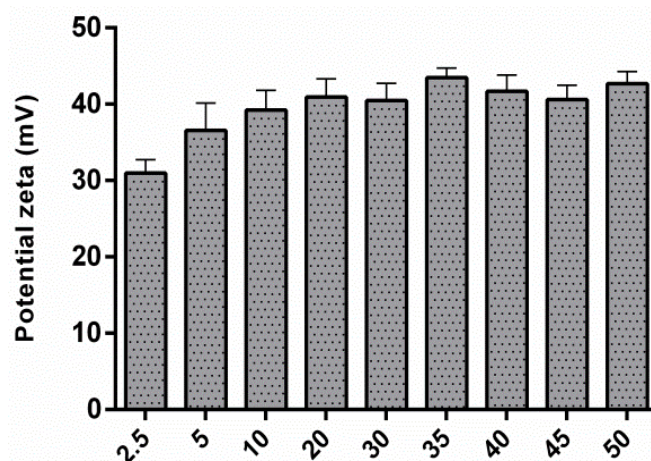


Figure 24. Zeta potential analysis for different N/P ratios of CS-MMW conjugated with sRNA.

The values of zeta potential were calculated with the data obtained from three independent measurements (mean \pm SD, n = 3).

As noted above, PEI and CS promote sRNA condensation at distinct N/P ratios, because they have very different characteristics that make them act in the different ways. For example, the shorter chains of PEI possess a higher charge density, and the polyanion is condensed but more exposed. Otherwise, in longer chains, as it is the case of CS, the charge density is decreased, and the polyanion is neutralized by the oppositely charged chains. Thus, it was observed that, while the highest density chains promoted higher degree of RNA compaction, the longer chains were more effective in complexation of the RNA molecule [121]. This is consistent with experimental results, PEI is more densely charged but has lower size than the CS.

The sRNA/CS particles seem to be one promising vehicle for RNA delivery because they revealed suitable size values, close to 300 nm, and exhibited positive zeta values in the relevant range of N/P ratios tested. A longer polycation with low charge density can induce a similar degree of condensation relatively to a shorter polycation with a high linear charge density. The accessibility of the positive charge and effects of charge matching may also favor an efficient condensation [121].

3.4 SEM

The morphology of the polyplexes under study was investigated by SEM, as illustrated in Figures 25 and 26. As apparent from the figure 25, the prepared PEI-SA, for instance, demonstrated spherical shape with average size of about 200-300 nm which is in agreement with the size values obtained from the DLS measurements.

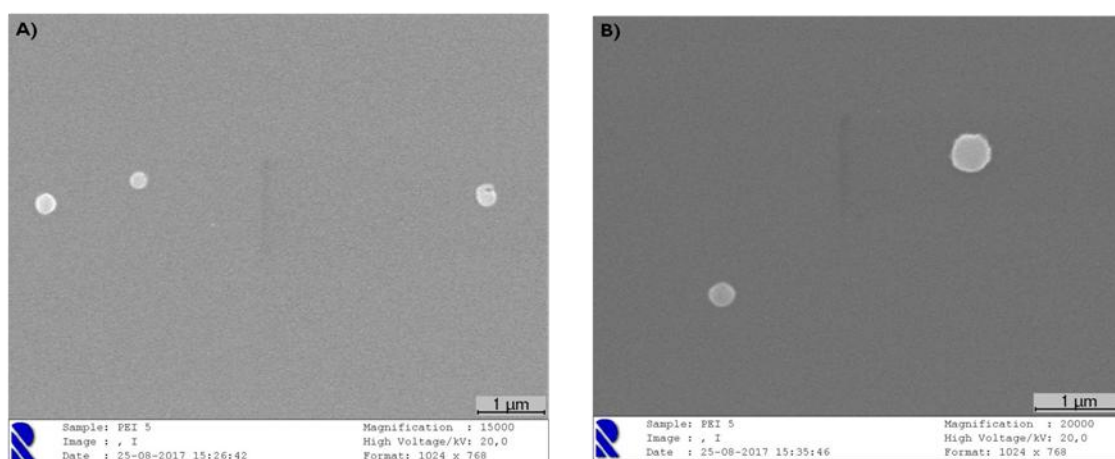


Figure 25. PEI-SA polyplexes obtained by simple complexation at pH 4.5 visualized by SEM.

(A) PEI-SA (N/P=5) - $D_1=326\text{nm}$; $D_2=254\text{nm}$; $D_3=350\text{nm}$, (B) PEI-SA (N/P=5) - $D_1=409\text{nm}$; $D_2=276\text{nm}$.

As well, the CS-SA polyplexes, in the figure 26, also demonstrated spherical shape with average size between 300 to 600 nm, which is also in accordance with the size values from the DLS measurements.

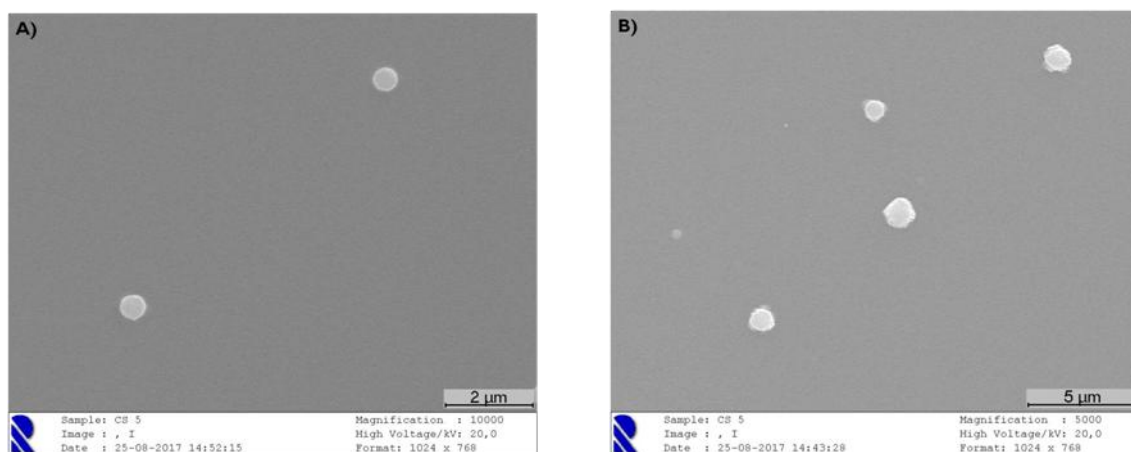


Figure 26. CS-SA polyplexes obtained by simple complexation at pH 4.5 visualized by SEM.

(A) CS-SA (N/P=5) - $D_1=545\text{nm}$; $D_2=510\text{nm}$, **(B)** CS-SA(N/P=5) - $D_1=428\text{nm}$; $D_2=416\text{nm}$; $D_3=386\text{nm}$.

The spherical shape is a feature of these polyplexes. Through electrostatic interactions, the polymer surrounds the therapeutic biomolecule. Comparatively, the PEI-SA polyplexes presented lower size - 200-300 nm - than the CS-SA polyplexes - 300-600 nm -, which may be due to the longer chain of CS, as previously described [121].

Additionally, the sizes obtained were slightly higher than the ones obtained by Pereira and co-workers, describing the preparation of nanoparticles with sizes between 100-300 nm. To achieve an efficient internalization by endocytic processes, the size of the polyplexes should be between 50 nm and 200 nm. In this case, the polymers chosen would be with the smallest sizes, closer to 200 nm, as they could also be more effective for lung cancer application. In fact, the large alveolar surface area is suited for drug absorption, and provides low thickened epithelial barrier, extensive vascularisation, and absence of first-pass effect, compared to other routes of administration. Thus, the nanoparticles are retained in the lungs, being able to release the drug in a sustained manner. In addition, particles smaller than 260 nm are less likely to suffer uptake by the macrophages and achieve efficient drug delivery [122].

3.5. Functionalization of PEI-SA and CS-SA with Lf

In addition to the successful functionalization of both polymers with SA, a second functionalization was attempted. The Lactoferrin (Lf) ligand was added to the particle with the purpose of targeting the lung cancer cells, since bronchial epithelial cells present receptors specific for Lf [98]. Thus, it is expected that with this functionalization, the particle can specifically interact with the cancer cells, thereby minimizing their interaction with healthy cells. The functionalization with Lf was accomplished using a common method that employs 2-iminothiolane hydrochloride as the sulfhydrylization reagent [123]. Based in the previous results of structural properties of the complexes, only the ratios with better sizes, the best encapsulation efficiency and the highest zeta potential values were prepared for the second functionalization. For PEI-SA-Lf the selected N/P ratios were 12.5; 15; 20 and 30, and for CS-SA-Lf the N/P ratios studied were 30; 35 and 40.

The SDS-PAGE was used to further confirm the surface capping of the terminal amines of the CS/PEI-SA with Lf. In the SDS-PAGE, the band observed at 75 KDa, indicates that Lf ligand was covalently attached to the PEI-SA and CS-SA (Figure 27).

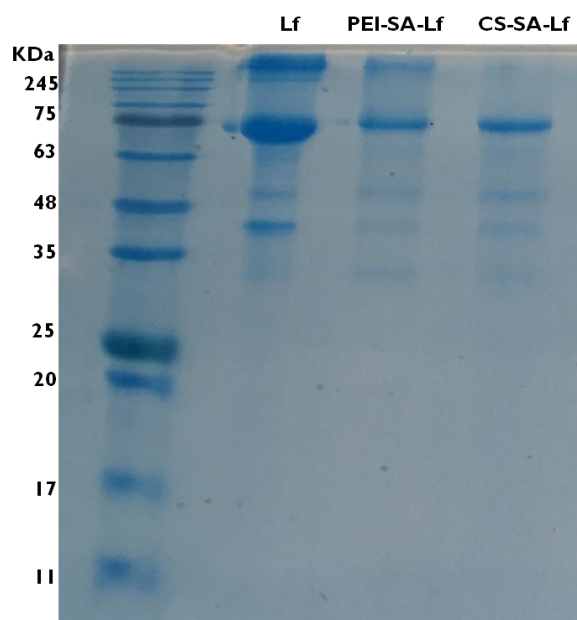


Figure 27. SDS-PAGE of PEI-SA-Lf and CS-SA-Lf.

After this second functionalization, the properties of the particles were also studied, and the N/P ratios with the better characteristics regarding size, zeta potential and encapsulation efficiency were for PEI-SA-Lf 20 and 30, and for CS were the 35 and 40 ratios, as represented in table 8. The second functionalization with the Lf, slightly affected the characteristics of the polyplexes, mainly in the size values. In general, for all N/P ratios the size is higher than in non-functionalized polyplexes, this is probably due to the presence of the Lf. Only the CS-SA-Lf kept the same size value comparatively with the non-functionalized polyplexes, with approximately 300 nm.

Relatively to the zeta potential values, both ratios of CS-SA-Lf showed higher values than other two PEI-SA-Lf N/P ratios. For CS-based systems, both 35 and 40 ratios presented similar behavior before and after functionalization with Lf, about 40 mV. In the PEI-SA-Lf polyplexes, the zeta potential values were slightly lower than the non-functionalized polyplexes.

On the contrary, in terms of encapsulation efficiency, PEI-SA-Lf was similar to PEI-SA. To the PEI-SA-Lf N/P ratio 20, the encapsulation value was 97.22% and in the same N/P ration of PEI-SA the efficiency was about 95%. In the ratio 30 of PEI-SA the difference is more evident, because the functionalized polyplexes showed 90.28% of encapsulation efficiency and the unmodified PEI-SA, presented a 97% of encapsulation efficiency. In the CS-SA-Lf ratios it was verified a slightly lower encapsulation efficiency (96% for ratio 35 and 88% for ratio 40) in comparison with the unmodified CS-SA (98% to 35 ratio and 90% to 40 ratio). Although there was a small difference, this is not significant to claim that functionalization had an influence on encapsulation efficiency.

Table 8. Polyplexes characterization.

Polyplexes	N/P ratio	Size (nm)	Zeta Potential (mV)	Encapsulation efficiency
PEI-SA-Lf	20	420 ± 1.16	19.37 ± 0.55	97.22 ± 4.81
	30	514.93 ± 16.87	25.43 ± 0.06	90.28 ± 1.96
CS-SA-Lf	35	317.7 ± 9.05	42.34 ± 1.46	96.35 ± 3.56
	40	658.65 ± 8.13	41.68 ± 2.20	88.94 ± 3.68

Thus, from the polyplexes developed in this work, after the functionalization with the Lf ligand, CS-SA-Lf polyplexes appear to be the most promising complexes for application in RNA delivery for therapy. Chiefly, the CS-SA-Lf N/P ratio 35, which exhibited the highest positive zeta values, to cross the negatively charged cell membrane, smaller size to an efficient internalization by endocytosis and, additionally, displays higher encapsulation efficiency, demonstrating that the protonated amine groups promoted electrostatic interactions with the negatively charged phosphate groups in RNA, neutralizing and completely surrounding the therapeutic molecule.

The use of these biopolymers has its advantages over other non-viral delivery systems for cancer cells, because these polymers are biodegradable, biocompatible, had low toxicity and immunogenicity. The reduction of non-specific biodistribution and the fact that the surface can readily be modified, lead to a high efficacy in the delivery of biopharmaceuticals into the specific cells/tissues. They also offer other advantages such as low production costs, high flexibility and easy quality control.

3.6. Preparation of PEI-SA-Lf-pre-miR-29b and CS-SA-Lf-pre-miR-29b

The pre-miR-29b-loaded complexes (PEI-SA-Lf/CS-SA-Lf) were prepared by electrostatic interactions that occur between the positively charged amine groups of the carriers and the phosphate groups of the pre-miR-29b [121]. The complexes PEI and CS were mixed with pre-miR-29b, using the ratios presented in the previous table, for the formation of pre-miR-29b-loaded complexes in acetate buffer at pH 4.5.

3.7. In vitro transfection and expression

3.7.1. Evaluation of DNMT1 protein knockdown induced by pre-miR-29-loaded complexes

The main goal of this work was to produce recombinant pre-miR-29 using the versatile *E. coli DH5 α* and to purify these pre-miRNAs by affinity chromatography aiming the preparation of polyplexes with polycations for a possible therapeutic application in lung cancer. Therefore, based in previously reported strategies [103], the effects of the target pre-miRNAs on the levels of DNMT1 were analyzed to evaluate their potential role on lung cancer therapeutics. This was investigated through the analysis of DNMT1 mRNA levels by RT-qPCR. For this purpose, H1299 cells were transfected with PEI-SA-Lf/pre-miR-29, CS-SA-Lf/pre-miR-29 using 10 nM of the target miRNA. After 48 hours of transfection, it was verified that the overexpression of recombinant pre-miR-29 in cells induced a decrease on the DNMT1 mRNA levels. In particular, for PEI-SA-Lf/pre-miR-29, the DNMT1 mRNA expression decreased approximately 36%, while for cells transfected with CS-SA-Lf/pre-miR-29, a decrease of 49% on DNMT 1 expression was obtained, when compared with untreated cells (Figure 29).

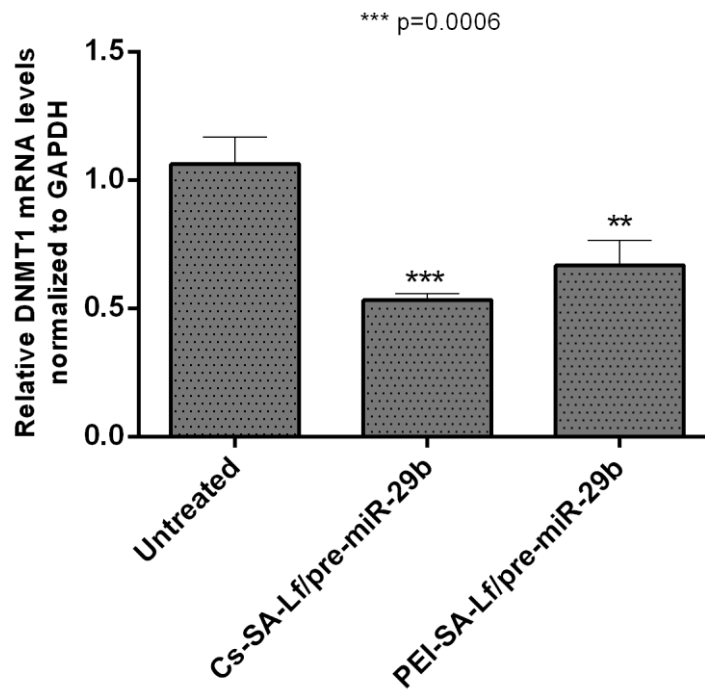


Figure 28. *In vitro* gene silencing effect of recombinant pre-miR-29b conjugated with PEI-SA-Lf and CS-SA-Lf on the DNMT1 mRNA levels, in H1299 cells normalized to GAPDH mRNA.

Untreated cells are control tests. Results presented are the mean of three independent tests.

Analyzing the graphic, the *in vitro* cellular uptake study showed that Lf with SA, conjugated with CS shows highly efficient in cell transfection, and induced a higher silencing effect on DNMT1 mRNA in comparison to the PEI conjugated with Lf and SA. With these results it was verified that DNMT1 is a direct target of pre-miR-29b, which was further confirmed by the downregulation of DNMT1 gene expression by polycations/pre-miR-29b *in vitro*.

This study provides a strong rationale for developing therapies that use recombinant pre-miR-29, alone or in combination with other treatments, to reactivate tumor suppressors and normalize aberrant patterns of methylation in lung cancer.

CHAPTER IV - Conclusions and Future Perspectives

The discovery of RNA interference was remarkable, being recognized that RNA is not a simply intermediate between DNA and proteins but a versatile molecule fundamental in the regulation of gene expression and in the control of numerous cellular processes. MiRNAs can be potentially involved in the origin and progression of diseases, emerging as interesting biopharmaceutical products. However, it was realized that obtaining ncRNAs drugs was not as straightforward as originally thought, thereby highlighting the need to develop efficient technologies for miRNAs recombinant production and purification.

This work focused on the preparation of pre-miR-29, as it was previously indicated its potential application as biopharmaceutical in lung cancer therapy. Actually, pre-miR-29 regulates the DNMT's levels, which could replacing the natural patterns of DNA methylation in non-small-cell lung cancer.

To address these issues, this project successfully established a new strategy to purify the recombinant pre-miR-29, coupled with the preparation of suitable non-viral systems for the targeted-delivery of pre-miR-29 to the lung cancer cells. The recombinant production was performed in a genetically modified organism, using the bacterium *E. coli DH5 α* , harboring a plasmid pBHSR1-RM-pre-miR-29, encoding human pre-miR-29. The previously optimized growth conditions for the *E. coli DH5 α* were applied in this process, being verified that the production of pre-miR-29 was suitable for these studies. Regarding the purification process, it was concluded that amino acid-based affinity chromatography can be considered as a promising strategy using the superporous arginine matrix support. Some different elution profiles were studied and the pre-miR-29 purification was more successful when the elution was performed by using a stepwise increasing NaCl gradient consisting in 100 mM, 130 mM and 500 mM, in 10 mM Tris-HCl buffer at pH 8.0. Although the purity degree was not optimal, the application of arginine as specific ligand in a superporous matrix, allowed the pre-miR-29 recovery under mild salt conditions, showing that this matrix can be a good alternative to purify pre-miR-29.

As a future strategy to improve the pre-miR-29 purification degree, some competition agents could be used in the mobile phase trying to achieve higher selectivity towards pre-miRNA. For example, considering the versatility of Ionic Liquids (IL), their use in competition studies could be carried out to achieve higher specificity, also combining with an optimization of different parameters (pH, temperature and salt concentration).

After the purification of the target molecule, the project addressed the development of delivery systems able to carry and deliver the pre-miR-29 to the target cells. The polymers PEI and CS were used in order to design a successful non-viral delivery system for small RNAs. The conjugation of PEI and CS with small RNAs was evaluated regarding their physicochemical characteristics, namely size, zeta potential, morphology and encapsulation efficiency. Both polyplexes demonstrated high loading capacity, small sizes and exhibited a strong positive charge on their surface. However, in comparison, CS appeared to have the most promising behavior, since it revealed higher values for zeta potential, which favor an efficient condensation due to the accessibility of the positive charge, as well demonstrated high encapsulation efficiency values in all studied ratios.

Considering the application of the pre-miR-29 in the lung cancer cells, these delivery systems were also functionalized with specific ligands. The Lf ligand was selected, once their receptor is expressed on the apical surface of bronchial epithelial cells. Thus, the inclusion of these ligands on the polyplex surface could facilitate their access and their interaction with target cells. The *in vitro* study demonstrated that PEI-SA-Lf and CS-SA-Lf could efficiently deliver the recombinant pre-miR-29 as a therapeutic agent to the lung cancer cells, and the cellular effect was verified, once the pre-miR-29 induced a decrease of DNMT1 mRNA levels on transfected cells. Specifically, the *in vitro* cellular uptake study showed that the system with Lf and SA conjugated with CS induced a decrease of about 49% in DNMT1 mRNA levels and the conjugation of PEI-SA-Lf induced a repression of approximately 36%. In general, these results suggest that PEI and CS conjugated with SA and Lf could represent a potentially promising and interesting therapeutic delivery strategy for targeting

recombinant pre-miR-29 to lung cancer cells. The decrease of the expression levels of DNMT1 by the pre-miR-29 suggests its potential therapeutic effect and indicates the possibility to induce a re-expression of tumor suppressor genes, such as FHIT and WWOX, which are frequently silenced by promoter methylation in lung cancer.

As a future perspective, the effects of the methylation changes on gene expression, and the mRNA expression levels of two TSGs, FHIT and WWOX, should be characterized and analyzed. The main obstacle for the systemic delivery of miRNAs for lung cancer therapy is to determine their uptake in specific cells. Moreover, the delivery strategy has to overcome several challenges related with miRNAs degradation by nucleases, renal clearance, failure to cross the capillary endothelium, ineffective endocytosis by target cells, and activation of the host immune responses. Thus, as future perspective it should be considered the preparation of different delivery systems, namely based on polymers, such as polymeric nanoparticles (e.g. Poly(lactic-co-glycolic acid)) and poloxamer micelles (Pluronic® block copolymers). Overall, the future development of miRNAs-based therapy will focus in the improvement of stability, delivery, and control of off target effects of miRNAs.

CHAPTER V - Bibliography

1. FIRE, A., S, X., et al. (1998). Potent and specific genetic interference by double-stranded RNA in *Caenorhabditis elegans*. *Nature*, 391, 806–811.
2. BURNETT, J. C., Rossi, J. J. (2012). RNA-Based Therapeutics: Current Progress and Future Prospects. *Chemistry & Biology*, 19, 60–71.
3. CHU, C., Rana, T. (2007). Small RNAs: Regulators and Guardians of the Genome. *Journal of cellular physiology*, 213, 412–419.
4. ZAMORE, P. et al. (2000). RNAi: double-stranded RNA directs the ATP-dependent cleavage of mRNA at 21 to 23 nucleotide intervals. *Cell*, 101, 25–33.
5. DOGINI, D. B., et al. (2014). The new world of RNAs. *Genetics and Molecular Biology*, 37, 285–293.
6. GOMES, A. Q., Nolasco, S., Soares, H. (2013). Non-Coding RNAs: Multi-Tasking Molecules in the Cell. *International Journal of Molecular Sciences*, 14, 16010–16039.
7. RAMACHANDRAN, P. V., Ignacimuthu, S. (2013). RNA interference - A silent but an efficient therapeutic tool. *Applied Biochemistry and Biotechnology*, 169, 1774–1789.
8. QURASHI, A., Jin, P. (2010). Small RNA-mediated gene regulation in neurodevelopmental disorders. *Current Psychiatry Reports*, 12, 154–161.
9. KIM, V. N. (2005). Small RNAs: classification, biogenesis, and function. *Molecules and cells*, 19, 1–15.
10. GAVRILOV, K., Saltzman, W. M. (2012). Therapeutic siRNA: Principles, challenges, and strategies. *Yale Journal of Biology and Medicine*, 85, 187–200.
11. ZHU, J. J., et al. (2013). Function of lncRNAs and approaches to lncRNA-protein interactions. *Science China Life Sciences*, 56, 876–885.

12. HARRIES, L. W. (2012). Long non-coding RNAs and human disease. *Biochemical Society Transactions*, 40, 902–906.
13. PEREIRA, P., et al. (2016). Affinity approaches in RNAi-based therapeutics purification. *Journal of Chromatography B*, 1021, 45–56.
14. SULLENGER, B. A., Gilboa, E. (2002). Emerging clinical applications of RNA. *Nature*, 418, 252–258.
15. BUMCROT, D., et al. (2006). RNAi therapeutics: a potential new class of pharmaceutical drugs. *Nature Chemical Biology*, 2, 711–719.
16. Milhavet, O., Gary, D., Mattson, M. (2003). RNA interference in biology and medicine. *Pharmacological reviews*, 55, 629–648.
17. SATOH, J. (2010). MicroRNAs and their therapeutic potential for human diseases: aberrant microRNA expression in Alzheimer's disease brains. *Journal of Pharmacological Sciences*, 114, 269–275.
18. BARTEL, D. P. (2004). MicroRNAs: Genomics, Biogenesis, Mechanism, and Function. *Cell*, 116, 281–297.
19. HAN, J., Lee, Y., Yeom, K. H. (2006). Molecular Basis for the Recognition of Primary microRNAs by the Drosha-DGCR8 Complex. *Cell*, 125, 887–901.
20. SELBACH, M., et al. (2008). Widespread changes in protein synthesis induced by microRNAs. *Nature*, 455, 58–63.
21. NILSEN, T. W. (2007). Mechanisms of microRNA-mediated gene regulation in animal cells. *Trends Genet*, 23, 243–249.
22. BRODERICK, J. A., Zamore, P. D. (2011). MicroRNA therapeutics. *Gene Therapy*, 18, 1104–1110.

23. DU, L., Pertsemlidis, A. (2011). Cancer and neurodegenerative disorders: Pathogenic convergence through microRNA regulation. *Journal of Molecular Cell Biology*, 3, 176–180.
24. GARZON, R., et al. (2009). MicroRNA 29b functions in acute myeloid leukemia. *Blood*, 114, 5331–5341.
25. PEKARSKY, Y., et al. (2006). Tcl1 expression in chronic lymphocytic leukemia is regulated by miR-29 and miR-181. *Cancer Research*, 66, 11590–11593.
26. NGUYEN, T., et al. (2011). Downregulation of microRNA-29c is associated with hypermethylation of tumor-related genes and disease outcome in cutaneous melanoma. *Epigenetics*, 6, 388–394.
27. XIONG, Y., et al. (2010). Effects of microrna-29 on apoptosis, tumorigenicity, and prognosis of hepatocellular carcinoma. *Hepatology*, 51, 836–845.
28. CUMMINS, J. M., et al. (2006). The colorectal microRNAome. *Proceedings of the National Academy of Sciences of the United States of America*, 103, 3687–3692.
29. LI, Y., et al. (2011). Progressive miRNA expression profiles in cervical carcinogenesis and identification of HPV-related target genes for miR-29. *Journal of Pathology*, 224, 484–495.
30. YANAIHARA, N., et al.(2006). Unique microRNA molecular profiles in lung cancer diagnosis and prognosis. *Cancer Cell*, 9, 189–198.
31. HE, Y., et al (2013). MicroRNA-29 family, a crucial therapeutic target for fibrosis diseases. *Biochimie*, 95, 1355–1359.
32. PEREIRA, P. et al. (2016). Recombinant pre-miR-29b for Alzheimer’s disease therapeutics. *Scientific Reports*, 6, 19946.
33. GONG, J., et al. (2013). The role, mechanism and potentially therapeutic application of microRNA-29 family in acute myeloid leukemia. *Cell Death and Differentiation*, 21, 1–13.

34. EDELMANN, F. T., Niedner, A., Niessing, D. (2013). Production of pure and functional RNA for in vitro reconstitution experiments. *Methods*, 65, 333–341.
35. LING, H., Fabbri, M., Calin, G. A. (2013). MicroRNAs and other non-coding RNAs as targets for anticancer drug development. *Nature Reviews Drug Discovery*, 12, 847–865.
36. BECKERT, B., Masquida, B. (2011). Synthesis of RNA by In Vitro Transcription. *Methods in Molecular Biology*, 703, 29–41.
37. HUANG, Y., et al. (2011). Construction and detection of expression vectors of microRNA-9a in BmN cells. *Journal of Zhejiang University. Science. B*, 12, 527–33.
38. MARTINS, R., Queiroz, J. A., Sousa, F. (2014). Ribonucleic acid purification. *Journal of Chromatography A*, 1355, 1–58.
39. PONCHON, L., Dardel, F. (2011). Large scale expression and purification of recombinant RNA in Escherichia coli. *Methods*, 54, 267–273.
40. LI, M. M., et al (2014). Rapid production of novel pre-MicroRNA agent hsa-mir-27b in escherichia coli using recombinant RNA technology for functional studies in mammalian cells. *Drug Metabolism and Disposition*, 42, 1791–1795.
41. SUZUKI, H., et al. (2009). Characterization of extracellular DNA production and flocculation of the marine photosynthetic bacterium *Rhodovulum sulfidophilum*. *Applied Microbiology and Biotechnology*, 84, 349–356.
42. PEREIRA, et al. (2016). Advances in time course extracellular production of human pre-miR-29b from *Rhodovulum sulfidophilum*. *Applied Microbiology and Biotechnology*, 100, 3723–3734.
43. ANDO, T., et al. (2004). Extracellular RNAs produced by a marine photosynthetic bacterium *Rhodovulum sulfidophilum*. *Nucleic Acids Symposium Series*, 48, 165–166.

44. ANDO, T., et al. (2006). Characterization of extracellular RNAs produced by the marine photosynthetic bacterium *Rhodovulum sulfidophilum*. *Journal of Biochemistry*, 139, 805–811.
45. WASSARMAN, K. M., Zhang, A., Storz, G. (1999). Small RNAs in *Escherichia coli*. *Trends in Microbiology*, 7, 37–45.
46. WEI, Z., et al. (2007). Studies on endotoxin removal mechanism of adsorbents with amino acid ligands. *Journal of Chromatography B*, 852, 288–292.
47. PEREIRA, P., et al. (2017). New insights for therapeutic recombinant human miRNAs heterologous production: *Rhodovulum sulfidophilum* vs *Escherichia coli*. *Bioengineered*, 0, 1–8.
48. CHOMCZYNSKI, P., Sacchi, N. (2006). The single-step method of RNA isolation by acid guanidinium thiocyanate-phenol-chloroform extraction: twenty-something years on. *Nature Protocols*, 1, 581–585.
49. EASTON, L. E., Shibata, Y., Lukavsky, P. J. (2010). Rapid, nondenaturing RNA purification using weak anion-exchange fast performance liquid chromatography. *Method*, 16, 647–53.
50. NOLL, B., et al. (2011). Purification of Small Interfering RNA Using Nondenaturing. *Nucleic Acid Therapeutics*, 21, 383–393.
51. KOUBEK, J., et al. (2015). Strong anion-exchange fast performance liquid chromatography as a versatile tool for preparation and purification of RNA produced by in vitro transcription. *Method*, 19, 1449–1459.
52. MCCARTHY, S. M., Gilar, M., Gebler, J. (2009). Reversed-phase ion-pair liquid chromatography analysis and purification of small interfering RNA. *Analytical Biochemistry*, 390, 181–188.

53. SOUSA, F., Prazeres, D. M. F., Queiroz, J. A. (2008). Affinity chromatography approaches to overcome the challenges of purifying plasmid DNA. *Trends in Biotechnology*, 26, 518–525.
54. SOUSA, A., et al. (2011). Successful application of monolithic innovative technology using a carbonyldiimidazole disk to purify supercoiled plasmid DNA suitable for pharmaceutical applications. *Journal of Chromatography A*, 1218, 8333–8343.
55. MARTINS, R., Queiroz, J. A., Sousa, F. (2011). Histidine affinity chromatography-based methodology for the simultaneous isolation of Escherichia coli small and ribosomal RNA. *Biomedical Chromatography*, 26, 781–788.
56. LOWE, C. R., Lowe, A. R., Gupta, G. (2001). New developments in affinity chromatography with potential application in the production of biopharmaceuticals. *Journal of Biochemical and Biophysical Methods*, 49, 561–574.
57. SOUSA, Â., Sousa, F., Queiroz, J. A. (2012). Advances in chromatographic supports for pharmaceutical-grade plasmid DNA purification. *Journal of Separation Science*, 35, 3046–3058.
58. MARTINS, R., et al. (2012). A new strategy for RNA isolation from eukaryotic cells using arginine affinity chromatography. *Journal of Separation Science*, 35, 3217–3226.
59. SOUSA, F., Cruz, C., Queiroz, J. A. (2010). Amino acids-nucleotides biomolecular recognition: From biological occurrence to affinity chromatography. *Journal of Molecular Recognition*, 23, 505–518.
60. PEREIRA, P., et al. (2014). Purification of pre-miR-29 by arginine-affinity chromatography. *Journal of Chromatography B: Analytical Technologies in the Biomedical and Life Sciences*, 951–952, 16–23.

61. AFONSO, A., et al. (2014). Purification of pre-miR-29 by a new O-phospho-l-tyrosine affinity chromatographic strategy optimized using design of experiments. *Journal of Chromatography A*, 1343, 119–127.
62. PEREIRA, P., et al. (2014). New approach for purification of pre-miR-29 using lysine-affinity chromatography. *Journal of Chromatography A*, 1331, 129–132.
63. JONES, D., Lundgren, H., Jay, F. (1976). The separation of ribonucleic acids from *Escherichia coli* on lysin-agarose. *Nucleic Acids Res.*, 3, 1569–1576.
64. SOUSA, Â., Sousa, F., Queiroz, J. A. (2012). Advances in chromatographic supports for pharmaceutical-grade plasmid DNA purification. *Journal of Separation Science*, 35, 3046–3058.
65. PFAUNMILLER, E. L., et al. (2013). Affinity monolith chromatography: A review of principles and recent analytical applications. *Analytical and Bioanalytical Chemistry*, 405, 2133–2145.
66. MALLIK, R., Hage, D. S. (2006). Affinity monolith chromatography. *Journal of Separation Science*, 29, 1686–1704.
67. PEREIRA, P., et al. (2014). Pharmaceutical-grade pre-miR-29 purification using an agmatine monolithic support. *Journal of Chromatography A*, 1368, 173–182.
68. GUSTAVSSON, P. E., Axelsson, A., Larsson, P. O. (1999). Superporous agarose beads as a hydrophobic interaction chromatography support. *Journal of Chromatography A*, 830, 275–284.
69. MAEDA, H., Nakamura, H., Fang, J. (2013). The EPR effect for macromolecular drug delivery to solid tumors: Improvement of tumor uptake, lowering of systemic toxicity, and distinct tumor imaging in vivo. *Advanced Drug Delivery Reviews*, 65, 71–79.

70. ZHU, J., et al. (2014). Progress in aptamer-mediated drug delivery vehicles for cancer targeting and its implications in addressing chemotherapeutic challenges. *Theranostics*, 4, 931–944.
71. AL-DOSARI, M. S., Gao, X. (2009). Nonviral Gene Delivery: Principle, Limitations, and Recent Progress. *The AAPS Journal*, 11, 671–681.
72. TOKATLIAN, T., Segura, T. (2010). siRNA applications in nanomedicine. *Wiley Interdisciplinary Reviews: Nanomedicine and Nanobiotechnology*, 2, 305–315.
73. PATHAK, A., Patnaik, S., Gupta, K. C. (2009). Recent trends in non-viral vector-mediated gene delivery. *Biotechnology Journal*, 4, 1559–1572.
74. PEREIRA, P., et al. (2016). Smart micelleplexes as a new therapeutic approach for RNA delivery. *Expert Opinion on Drug Delivery*, 14, 353–371.
75. MORILLE, M., et al. (2008). Progress in developing cationic vectors for non-viral systemic gene therapy against cancer. *Biomaterials*, 29, 3477–3496.
76. CHEN, J., Xie, J. (2012). Progress on RNAi-based molecular medicines. *International Journal of Nanomedicine*, 7, 3971–3980.
77. HART, S. L. (2010). Multifunctional nanocomplexes for gene transfer and gene therapy. *Cell Biology and Toxicology*, 26, 69–81.
78. ZHANG, Y., Wang, Z., Gemeinhart, R. A. (2013). Progress in microRNA delivery. *Journal of Controlled Release*, 172, 962–974.
79. KAFIL, V., Omid, Y. (2011). Cytotoxic impacts of linear and branched polyethylenimine nanostructures in A431 cells. *BioImpacts*, 1, 23–30.
80. HAO, S., et al. (2015). Candesartan-graft-polyethyleneimine cationic micelles for effective co-delivery of drug and gene in anti-angiogenic lung cancer therapy. *Biotechnology and Bioprocess Engineering*, 20, 550–560.

81. TARATULA, O., et al. (2009). Surface-engineered targeted PPI dendrimer for efficient intracellular and intratumoral siRNA delivery. *Journal of Controlled Release*, 140, 284–293.
82. SU, W. P., et al. (2012). PLGA nanoparticles codeliver paclitaxel and Stat3 siRNA to overcome cellular resistance in lung cancer cells. *International Journal of Nanomedicine*, 7, 4269–4283.
83. LI, P., et al. (2011). A novel cationic liposome formulation for efficient gene delivery via a pulmonary route. *Nanotechnology*, 22, 245104.
84. KABANOV, A., Zhu, J., Alakhov, V. (2005). Pluronic Block Copolymers for Gene Delivery. *Advances in Genetics*, 53, 231–261.
85. HAN, Y., et al. (2014). Co-delivery of plasmid DNA and doxorubicin by solid lipid nanoparticles for lung cancer therapy. *International Journal of Molecular Medicine*, 34, 191–196.
86. CONDE, J., et al. (2013). In vivo tumor targeting via nanoparticle-mediated therapeutic siRNA coupled to inflammatory response in lung cancer mouse models. *Biomaterials*, 34, 7744–7753.
87. NIMESH, S., Chandra, R. (2009). Polyethylenimine nanoparticles as an efficient in vitro siRNA delivery system. *European Journal of Pharmaceutics and Biopharmaceutics*, 73, 43–49.
88. LI, N., Yang, X., Zhai, G., Li, L. (2010). Multifunctional pluronic/poly(ethylenimine) nanoparticles for anticancer drug. *Journal of Colloid and Interface Science*, 350, 117–125.
89. AKINC, A., et al. (2005). Exploring polyethylenimine-mediated DNA transfection and the proton sponge hypothesis. *Journal of Gene Medicine*, 7, 657–663.

90. BROMBERG, L., et al. (2009). Guanidinylated polyethyleneimine-polyoxypropylene-polyoxyethylene conjugates as gene transfection agents. *Bioconjugate Chemistry*, 20, 1044–1053.
91. HUWYLER, J., Wu, D., Pardridge, W. M. (1996). Brain drug delivery of small molecules using immunoliposomes. *Proceedings of the National Academy of Sciences of the United States of America*, 93, 14164–9.
92. DUCEPPE, N., Tabrizian, M. (2010). Advances in using chitosan-based nanoparticles for in vitro and in vivo drug and gene delivery. *Expert opinion on drug delivery*, 7, 1191–1207.
93. TAE, H. K., et al. (2005). Synergistic effect of poly(ethylenimine) on the transfection efficiency of galactosylated chitosan/DNA complexes. *Journal of Controlled Release*, 105, 354–366.
94. RUDZINSKI, W. E., Aminabhavi, T. M. (2010). Chitosan as a carrier for targeted delivery of small interfering RNA. *International Journal of Pharmaceutics*, 399, 1–11.
95. GERMERSHAUS, O., et al. (2008). Gene delivery using chitosan, trimethyl chitosan or polyethylenglycol-graft-trimethyl chitosan block copolymers: Establishment of structure-activity relationships in vitro. *Journal of Controlled Release*, 125, 145–154.
96. SARVAIYA, J., Agrawal, Y. K. (2015). Chitosan as a suitable nanocarrier material for anti-Alzheimer drug delivery. *International Journal of Biological Macromolecules*, 72, 454–465.
97. XIE, Y. T., et al. (2012). Brain-targeting study of stearic acid-grafted chitosan micelle drug-delivery system. *International Journal of Nanomedicine*, 7, 3235–3244.

98. PANDEY, V., Gajbhiye, K. R., Soni, V. (2015). Lactoferrin-appended solid lipid nanoparticles of paclitaxel for effective management of bronchogenic carcinoma. *Drug delivery*, 22, 199–205.
99. SIEGEL, R., et al. (2014). Cancer statistics, 2014. *CA: a Cancer Journal for Clinicians*, 64, 9–29.
100. BELINSKY, S. a. (2015). Unmasking the Lung Cancer Epigenome. *Annual Review of Physiology*, 77, 453–474.
101. FORTUNATO, O., et al. (2014). Therapeutic Use of MicroRNAs in Lung Cancer. *BioMed Research International*, 2014, 1–8.
102. SINGH, D. K., Bose, S., Kumar, S. (2016). Regulation of expression of microRNAs by DNA methylation in lung cancer. *Biomarkers*, 21, 589–599.
103. FABBRI, M., et al. (2007). MicroRNA-29 family reverts aberrant methylation in lung cancer by targeting DNA methyltransferases 3A and 3B. *Proceedings of the National Academy of Sciences of the United States of America*, 104, 15805–10.
104. ULIVI, P., et al. (2006). p16INK4A and CDH13 hypermethylation in tumor and serum of non-small cell lung cancer patients. *Journal of Cellular Physiology*, 206, 611–615.
105. FABBRI, M., et al. (2005). WWOX gene restoration prevents lung cancer growth in vitro and in vivo. *Proceedings of the National Academy of Sciences of the United States of America*, 102(43), 15611–6.
106. SUZUKI, M., et al. (2004). RNA Interference-Mediated Knockdown of DNA Methyltransferase 1 Leads to Promoter Demethylation and Gene Re-Expression in Human Lung and Breast Cancer Cells. *Cancer Research*, 64, 3137–3143.
107. PAO, W., Girard, N. (2011). New driver mutations in non-small-cell lung cancer. *The Lancet Oncology*, 12, 175–180.

108. KORPANTY, G. J., et al. (2014). Biomarkers that currently affect clinical practice in lung cancer: EGFR, ALK, MET, ROS-1, and KRAS. *Frontiers in Oncology*, 4, 1–27.
109. MAO, S., Sun, W., Kissel, T. (2010). Chitosan-based formulations for delivery of DNA and siRNA. *Advanced Drug Delivery Reviews*, 62, 12–27.
110. HUH, M. S., et al. (2010). Tumor-homing glycol chitosan/polyethylenimine nanoparticles for the systemic delivery of siRNA in tumor-bearing mice. *Journal of Controlled Release*, 144, 134–143.
111. MEL'NIKOVA, Y. S., Lindman, B. (2000). pH-controlled DNA condensation in the presence of dodecyldimethylamine oxide. *Langmuir*, 16, 5871–5878.
112. DE SMEDT, S. C., Demeester, J., Hennink, W. E. (2000). Cationic polymer based gene delivery systems. *Pharmaceutical Research*, 17, 113–126.
113. PONCHON, L., Dardel, F. (2007). Recombinant RNA technology: the tRNA scaffold. *Nature Methods*, 4, 571–576.
114. YARUS, M., Widmann, J. J., Knight, R. (2009). RNA-amino acid binding: A stereochemical era for the genetic code. *Journal of Molecular Evolution*, 69, 406–429.
115. JANAS, T., et al. (2010). Simple, recurring RNA binding sites for L-arginine. *RNA (New York, N.Y.)*, 16, 805–816.
116. PEREIRA, P., et al. (2017). New insights for therapeutic recombinant human miRNAs heterologous production: *Rhodovulum sulfidophilum* vs *Escherichia coli*. *Bioengineered*, 0, 1–8.
117. SRISAWAT, C., Engelke, D. R. (2001). Streptavidin aptamers: Affinity tags for the study of RNAs and ribonucleoproteins. *RNA Society*, 7, 632–641.

118. BONNET, M. E., Erbacher, P., Bolcato-Bellemin, A. L. (2008). Systemic delivery of DNA or siRNA mediated by linear polyethylenimine (L-PEI) does not induce an inflammatory response. *Pharmaceutical Research*, 25, 2972–2982.
119. HAGERMAN, P. J. (1997). Flexibility of RNA. *Annual Review of Biophysics and Biomolecular Structure*, 26, 139–156.
120. KUNATH, K., et al. (2003). Low-molecular-weight polyethylenimine as a non-viral vector for DNA delivery: Comparison of physicochemical properties, transfection efficiency and in vivo distribution with high-molecular-weight polyethylenimine. *Journal of Controlled Release*, 89, 113–125.
121. PEREIRA, P., et al. (2012). Characterization of polyplexes involving small RNA. *Journal of Colloid and Interface Science*, 387, 84–94.
122. AZARMI, S., Roa, W. H., Löbenberg, R. (2008). Targeted delivery of nanoparticles for the treatment of lung diseases. *Advanced Drug Delivery Reviews*, 60, 863–875.
123. HUANG, R., et al. (2009). Brain-Targeting Mechanisms of Lactoferrin-Modified DNA-Loaded Nanoparticles. *Journal of Cerebral Blood Flow & Metabolism*, 29, 1914–1923.